REPORT

Internal Repair of Pipelines
Review & Evaluation of Internal Pipeline Repair Trials Report

Reporting Period:
September 30, 2003 through June 30, 2004

Principal Authors:
Robin Gordon, Bill Bruce, Ian Harris, Dennis Harwig, George Ritter,
Bill Mohr, Matt Boring, Nancy Porter, Mike Sullivan, and Chris Neary

Report Issued: September 2004

EWi ®

MATERIALS JOINING TECHNOLOGY

DISCLAIMER

This report was prepared as an account of work sponsored by an agency of the United States Government. Neither the United States Government nor any agency thereof, nor any of their employees, makes any warranty, express or implied, or assumes any legal liability or responsibility for the accuracy, completeness, or usefulness of any information, apparatus, product, or process disclosed or represents that its use would not infringe privately owned rights. Reference herein to otherwise does not necessarily constitute or imply its endorsement, recommendation, or favoring by the United States Government or any agency thereof. The views and opinions of authors expressed herein do not necessarily state or reflect those of the United States Government or any agency hereof.

Measurement Units -- SI Metric System of Units are the primary units of measure for this report followed by their U.S. Customary Equivalents in parentheses ( ).

Note: SI is an abbreviation for "Le Systeme International d'Unites."

ABSTRACT

The two broad categories of fiber-reinforced composite liner repair and deposited weld metal repair technologies were reviewed and evaluated for potential application for internal repair of gas transmission pipelines. Both are used to some extent for other applications and could be further developed for internal, local, structural repair of gas transmission pipelines.

Evaluation trials were conducted on pipe sections with simulated corrosion damage repaired with glass fiber-reinforced composite liners, carbon fiber-reinforced composite liners, and weld deposition. Additional un-repaired pipe sections were evaluated in the virgin condition and with simulated damage. Hydrostatic failure pressures for pipe sections repaired with glass fiber-reinforced composite liner were only marginally greater than that of pipe sections without liners, indicating that this type of liner is generally ineffective at restoring the pressure containing capabilities of pipelines. Failure pressure for pipe repaired with carbon fiber-reinforced composite liner was greater than that of the un-repaired pipe section with damage, indicating that this type of liner is effective at restoring the pressure containing capability of pipe. Pipe repaired with weld deposition failed at pressures lower than that of un-repaired pipe in both the virgin and damaged conditions, indicating that this repair technology is less effective at restoring the pressure containing capability of pipe than a carbon fiber-reinforced liner repair.

Physical testing indicates that carbon fiber-reinforced liner repair is the most promising technology evaluated to-date. Development of a comprehensive test plan for this process is recommended for use in the next phase of this project.

TABLE OF CONTENTS

LIST OF TABLES

LIST OF GRAPHICAL MATERIALS

LIST OF EQUATIONS

1.0 - INTRODUCTION

Repair methods that can be applied from the inside of a gas transmission pipeline (i.e., trenchless methods) are an attractive alternative to conventional repair methods since pipeline excavation is precluded. This is particularly true for pipelines in environmentally sensitive and highly populated areas. Several repair methods that are commonly applied from the outside of the pipeline are, in theory, directly applicable from the inside. However, issues must be addressed such as development of the required equipment to perform repairs remotely and the mobilization of said equipment through the pipeline to areas that need to be repaired. In addition, several additional repair methods that are commonly applied to other types of pipelines (e.g., gas distribution lines, water lines, etc.) have potential applicability, but require further development to meet the requirements for repair of gas transmission pipelines.

Gas transmission pipeline repair by direct deposition of weld metal, or weld deposition repair, is a proven technology that can be applied directly to the area of wall loss (e.g., external repair of external wall loss - Figure 1) or to the side opposite to the wall loss (e.g., external repair of internal wall loss - Figure 2).

Figure 1 - Installation of a Full-Encirclement Repair Sleeve

Figure 2 - External Weld Deposition Repair of Internal Wall Loss in 90º Elbow

There are no apparent technical limitations to applying this repair method to the inside of an out-of-service pipeline. It is direct, relatively inexpensive to apply, and requires no additional materials beyond welding consumables. However, application of this repair method to the inside of an in-service pipeline would require that welding be performed in a hyperbaric environment. Deposited weld metal repairs are also used to repair circumferentially oriented planar defects (e.g., intergranular stress corrosion cracks adjacent to girth welds) in the nuclear power industry. Remote welding has been developed primarily to meet needs in the nuclear power industry, though working devices have been built for other applications, including repair of gas transmission pipelines. An example of such equipment is shown in Figure 3.

Figure 3 - Osaka Gas System for Remote Robotic Internal Repair of Root Weld Defects in Gas Transmission Pipelines

Fiber-reinforced composite repairs are becoming widely used as an alternative to the installation of welded, full-encirclement sleeves for repair of gas transmission pipelines. These repairs typically consist of glass fibers in a polymer matrix material bonded to the pipe using an adhesive. Adhesive filler is applied to the defect prior to installation to allow load transfer to the composite material. The primary advantage of these repair products over welded, full-encirclement sleeves is the fact that welding is precluded. An illustration of the most commonly used of the fiber-reinforced composite devices, Clock Spring®, is shown in Figure 4.
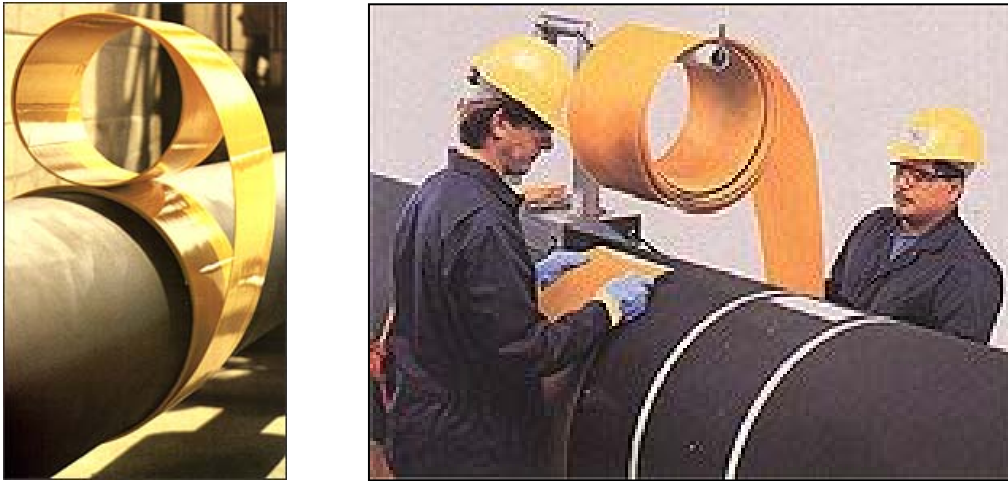
Figure 4 - Clock Spring® Fiber-Reinforced Composite Device for Pipeline Repair

A variety of liners are commonly used for repair of other types of pipelines (e.g., gas distribution lines, sewers, water mains, etc.). Of these, the three that are potentially applicable to internal repair of gas transmission pipelines are sectional liners, cured-in-place liners, and fold-and-formed liners. Sectional liners are typically 0.9 m (3 ft.) to 4.6 m (15 ft.) in length and are installed only in areas that require repairs. Cured-in-place liners and fold-and-formed liners are typically applied to an entire pipeline segment. Cured-in-place liners are installed using the inversion process, while fold-and-formed liners are pulled into place and then inverted so that they fit tightly against the inside of the pipe. The installation of a sectional liner is illustrated in Figure 5.

1. Liner wrapped around shroud packer.

2. Liner winched into position.

3. Packer pressurized with water.

4. After curing, packer is withdrawn.

Sectional Liner

Defect

Shroud Packer
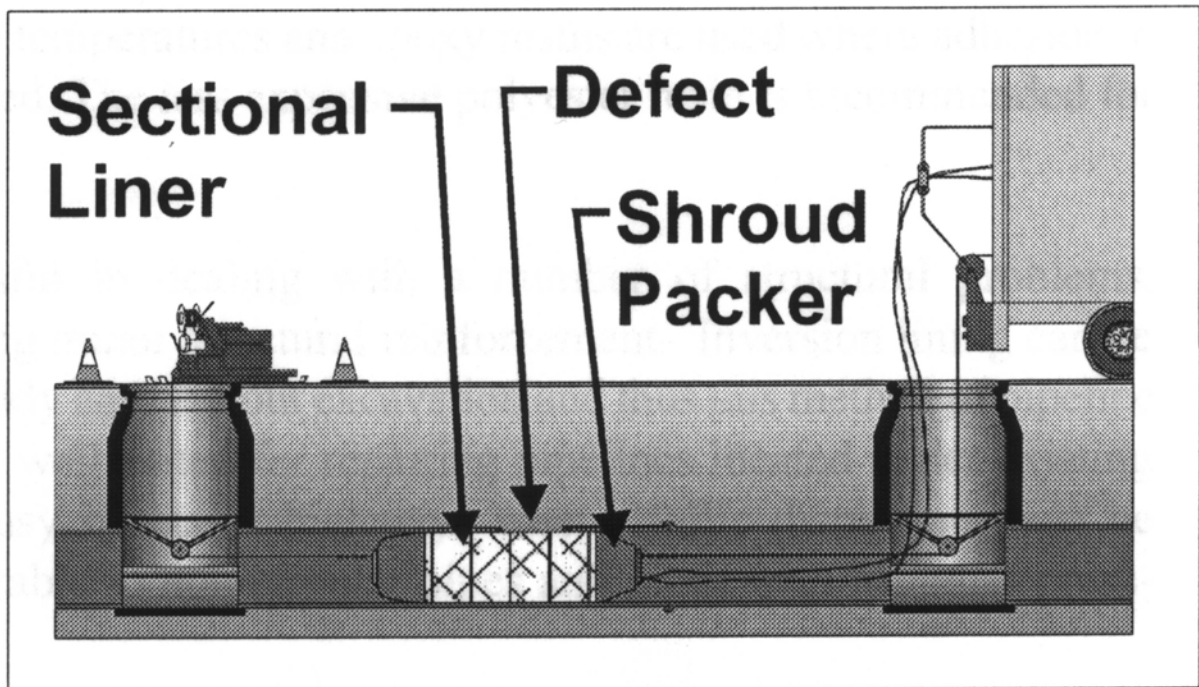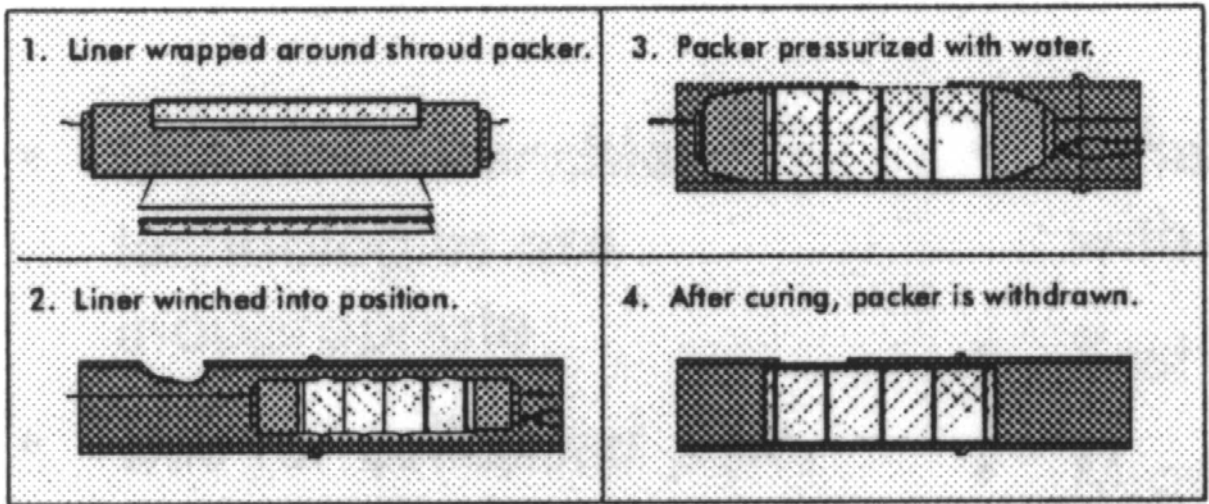
Figure 5 - Installation of a Sectional Liner in Low-Pressure Pipeline

2.0 - EXECUTIVE SUMMARY

The two broad categories of deposited weld metal repair and fiber-reinforced composite liner repair technologies were reviewed for potential application for internal repair of gas transmission pipelines. Both are used to some extent for other applications and could be further developed for internal, local, structural repair of gas transmission pipelines. Both of these repair technologies can easily be applied out-of-service and both require excavation prior to repair.

The most frequent cause for repair of gas transmission pipelines was identified as external, corrosion-caused loss of wall thickness. The most commonly used in-service method for repair is externally welding on a full-encirclement steel sleeve. Weld deposition repair is also a proven technology that can be applied directly to the area of wall loss. There are no apparent limitations to applying this repair technology to the outside of an out-of-service pipeline. Repairing the inside of an in-service pipeline, however, would require that welding be conducted in a hyperbaric environment, which would require extensive research to develop.

External corrosion can be repaired by applying adhesive to the defect and wrapping a fiber-reinforced composite liner material around the outside diameter of the pipeline. Fiber-reinforced composite liner repairs are becoming widely used to repair pipeline both in- and out-of-service as an alternative to welding. Three liners that are potentially applicable to internal repair of pipelines are sectional liners, cured-in-place liners, and fold-and-formed liners.

A test program was developed for both deposited weld deposition repair and fiber-reinforced composite liner repair. Areas of simulated damage were introduced into pipe sections using methods previously developed at EWI. These damaged pipe sections were then repaired with both weld deposition and fiber-reinforced composite liner repairs. The repaired pipe sections were then hydrostatically pressure tested until rupture to establish performance data for both repair processes. Additionally, un-repaired pipe sections in the virgin (i.e., undamaged) condition and with simulated corrosion damage were hydrostatically tested until rupture, therefore, baseline performance data was established to enable an apples-to-apples comparison of all performance data.

Glass fiber-reinforced composite liners were hydrostatically tested in small-scale pipe sections with simulated damage. Unlined, small-scale pipe sections with simulated damage were also hydrostatically tested until rupture. The pipe sections with glass fiber-reinforced liners failed at pressures only marginally greater than the pipes with no liners, indicating that the glass fiber-reinforced liners are generally ineffective at restoring the pressure containing capabilities of pipelines. Postmortem results indicate that a fiber-reinforced composite liner material that is more elastic would more effectively reinforce steel pipelines, thus allowing the liner to carry its share of the load without putting the interface between the liner and the steel pipe in tension.

Engineering analysis determined that a composite liner with a high fiber modulus and shear strength is required for composite liners to resist the types of shear stresses that can occur when external corrosion continues to the point where only the liner carries the stresses from the internal pressure in the pipe. Realistic combinations of composite material and thickness were analytically determined for use in a carbon fiber-reinforced liner system that EWI developed. Failure pressure for full-scale pipe repaired with the carbon fiber-reinforced composite liner was greater than that of the un-repaired pipe section with damage, indicating that the carbon fiber-reinforced liners are effective at restoring the pressure containing capabilities of gas transmission pipelines.

Specimens of virgin pipe material had the highest hydrostatic burst pressures. The pipe section with simulated corrosion damage repaired with a carbon fiber-reinforced liner had the next highest burst pressure. The specimens of un-repaired pipe with simulated corrosion damage had the third highest burst pressures. The pipe section with simulated corrosion damage repaired with weld deposition exhibited the lowest burst pressure.

Physical testing clearly indicates that carbon fiber-reinforced liner repair is the most promising technology evaluated to-date. Development of a comprehensive test plan for this process is recommended for use in the field demonstration portion of this program.

3.0 - EXPERIMENTAL

Following is a description of all experimental methods used during the development and evaluation of the internal pipeline repair technologies of fiber-reinforced liners and weld deposition.

3.1 - Fiber-Reinforced Liner Repair Trials

Several potentially useful commercial fiber-reinforced composite liner products are directly applicable to internal repair. The initial test program focused on a modified Wellstream-Haliburton/RolaTube product, which was a bi-stable reeled composite material used to make strong, lightweight, composite pipes and pipe linings (Figure 6). When unreeled, it changes shape from a flat strip to an overlapping circular pipe liner that is pulled into position. Following deployment, the longitudinal seam was welded with an adhesive that was activated and cured by induction heating. One example of this product is 100 mm (4 in.) diameter by 2.5 mm (0.10 in.) thick and is said to have a 5.9 MPa (870 psi) short-term burst pressure.
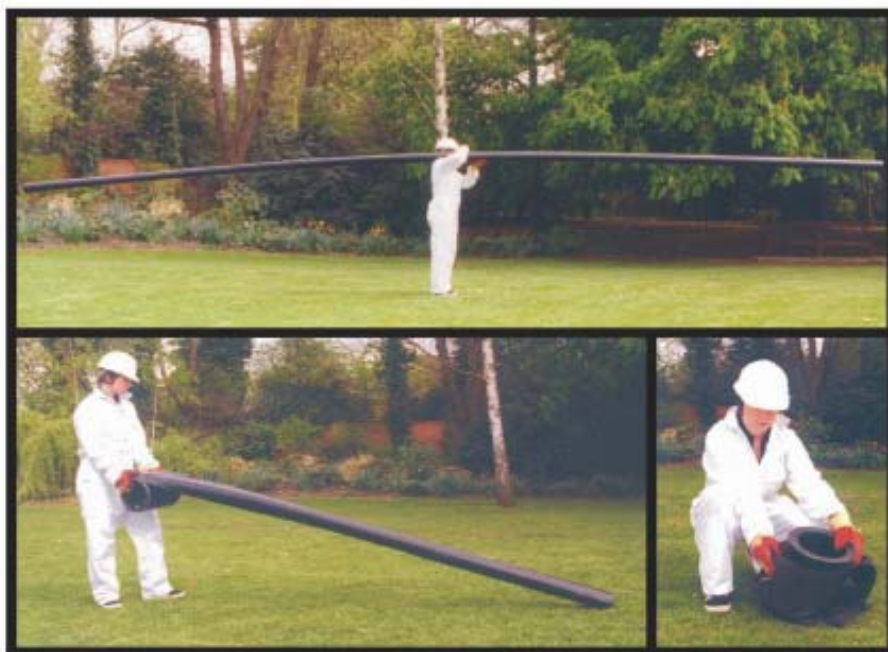
Figure 6 - RolaTube Bi-Stable Reeled Composite Material

For the initial trials, RolaTube developed a modified version of the bi-stable reeled composite product, which uses nine plies of a glass-polypropylene material in the form of overlapping, pre-pregnated tapes of unidirectional glass and polymer. Glass-high density polyethylene (HDPE) material was also considered. The glass-polypropylene material was selected after problems

bonding the glass-HDPE material to steel were encountered. Heat and pressure were used to consolidate the plies glass-polypropylene material into a liner (Figure 7). The resulting wall thickness of the liner is 2.85 mm (0.11 in.).

Figure 7 - Lay-Up and Forming of Fiber-Reinforced Composite Liner

A supply of 114.3 mm (4.5 in.) outside diameter (OD) by 4 mm (0.156 in.) wall thickness, API 5L Grade B pipe material was procured and cut into four 1.2 m (4 ft.) long sections. After the inside surface was degreased, lengths of lining were installed into two of the pipe sections (Figure 8).

Figure 8 - Insertion of Liner into 114.3 mm (4.5 in.) Diameter Pipe

The installation process consisted of inserting a silicon rubber bag inside the liner (Figure 9) and locating the liner inside the pipe. The silicon bag was then inflated to press the liner against the pipe wall.

Figure 9 - Silicon Rubber Bag Inserted into Liner

For these experiments, the entire pipe sections were then heated to 200°C (392°F) in an oven (Figure 10) to fuse the liner to the pipe wall.
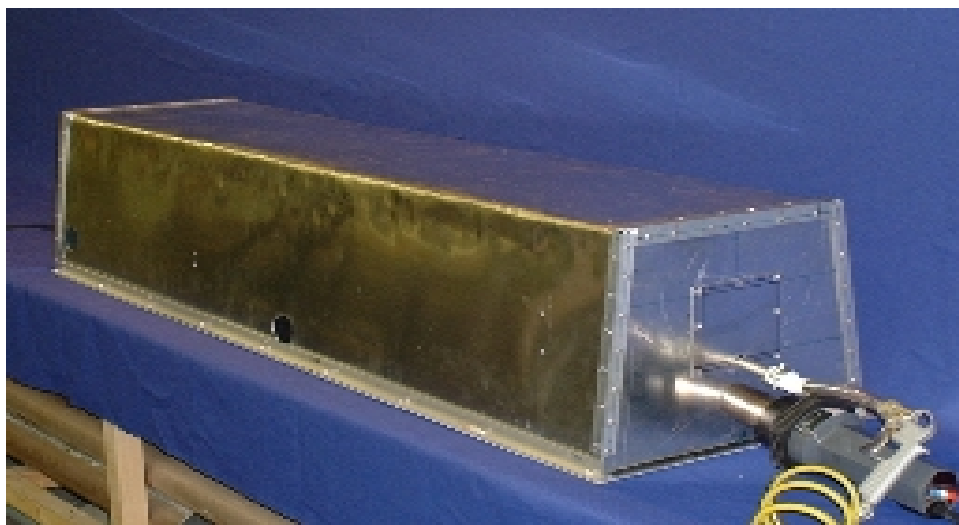
Figure 10 - Oven Used to Heat Pipe and Liner to 200°C (392°F)

Possible choices for liner installation in the field include infrared (IR) heaters on an expansion pig or a silicon bag inflated using hot air. An installed liner is shown in Figure 11.
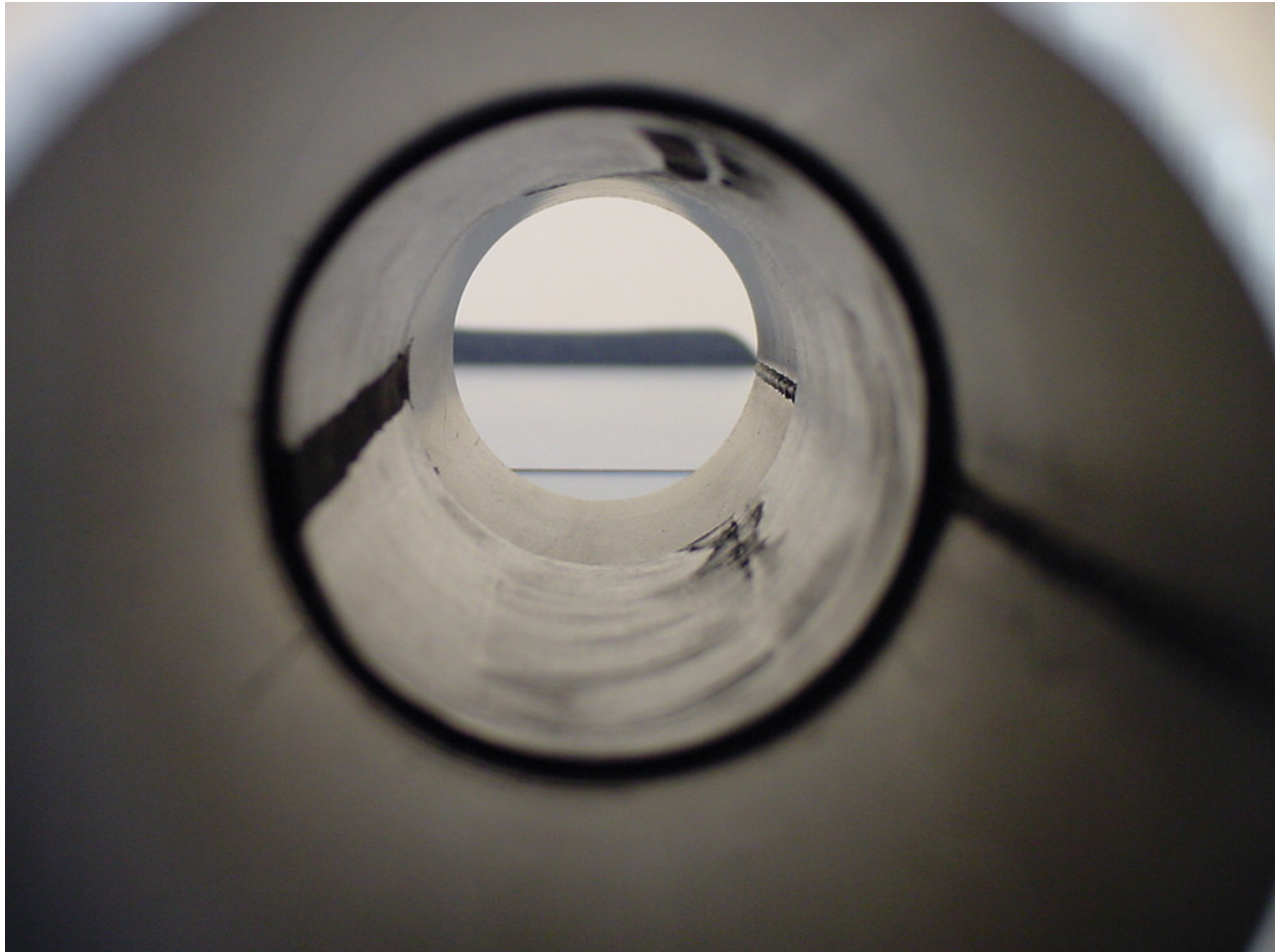
Figure 11 - Liner Inserted into Center of 114.3 mm (4.5 in.) Diameter Pipe

Using the RSTRENG software[1], dimensions of simulated general corrosion and a deep, isolated corrosion pit both with a 30% reduction in burst pressure were calculated then introduced into pipe sections with a milling machine. Using an end mill, long shallow damage representative of general corrosion (Figure 12) was introduced into one pipe section lined with fiber-reinforced composite liner and one without.

Figure 12 - Long, Shallow Simulated Corrosion Damage

Using an end mill with rounded corners, short, deep damage representative of a deep isolated corrosion pit (Figure 13) was introduced into the second pair of pipe sections; one lined, one not lined.
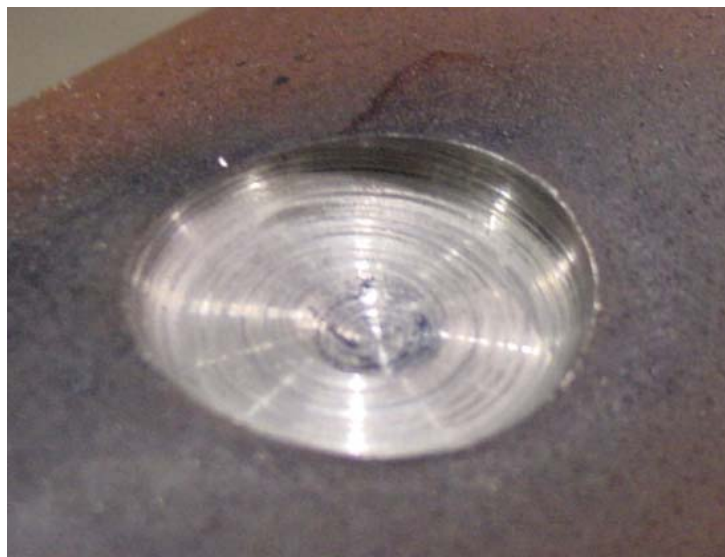
Figure 13 - Short, Deep Simulated Corrosion Damage

End caps were then welded to all four pipe sections as shown in Figure 14. Following the installation of end caps, all four pipe sections were hydrostatically pressurized to failure.

Figure 14 - 114.3 mm (4.5 in.) Diameter Pipe Section with End Caps Welded and Simulated Corrosion Damage

Using pipe sections with simulated corrosion damage, EWI hydrostatically tested a pipe section that was repaired with a carbon fiber-reinforced liner, which was fabricated in-house. EWI procured raw carbon fiber material and fabricated a 11.42 mm (0.45 in.) thick reinforcement patch using a "wet lay-up" process with a vinylester resin system. For the carbon fiber-reinforced liner repair simulation, a 508 mm (20 in.) diameter by 6.35 mm (0.25 in.) wall, API 5LX-52 pipe section was used (Figure 15).

Figure 15 - 508 mm (20 in.) Diameter API 5L-X52 Pipe Section Used for Carbon Fiber Liner Repair Test

With a ball end mill, long shallow damage representative of general corrosion was introduced into the pipe section. The simulated defect was 127 mm (5 in.) long and 3.45 mm (0.136 in.) deep (Figure 16) and effectively reduces the wall thickness down to 54%. The predicted burst pressure for this pipe material with a similar un-repaired defect is 6.72 MPa (974 psi).

Figure 16 - Simulated Corrosion Defect for Carbon Fiber Liner Repair Test in 508 mm (20 in.) Diameter Pipe

The raw materials used to create the patch were a standard 6K-tow, 5-harness weave carbon fiber fabric and a vinylester resin, catalyzed with methyl ethyl ketone peroxide (MEKP) and promoted with cobalt naphthenate. The resin had a gel time of 1.0 - 1.5 hours. The fabric was cut to give a quasi-isotropic lay-up with +/- 45 degrees for the outer layers, interleaved with 0 - 90 degree layers. A 567 g (20 oz.) woven roving, glass fabric outer layer was employed for the outer face (i.e., on the inside diameter of the patch). The inner glass face (i.e., outside diameter of the patch) was included to act as a galvanic corrosion barrier between the carbon fiber composite and the steel.

The composite patch was fabricated using a wet lay-up process followed by vacuum bagging. To develop the technique, the first trial was a flat panel, approximately 254 mm (10 in.) by 254 mm (10 in.). It was determined that additional layers of fabric were needed to increase section thickness. This was accomplished by including extra 0 - 90 degree internal layers of the semi-circular patch.

The half-round composite patch had an outside diameter that matched the internal diameter of the pipe section. The patch was 711 mm (28 in.) in length, 254 mm (10 in.) wide, by 11.42 mm (0.45 in.) thick. The semi-circular patch lay-up consisted of 27 layers; layers 1 and 27 were glass woven roving. The remainder consisted of alternating layers of +/- 45 degree and 0 - 90 degree (fiber orientation) to produce the patch (Table 1). A semi-circular mold was produced from a cut half-round of 20-inch pipe (Figure 17). Figure 18 shows the dry pack of quasi-isometric fiber build. Figure 19 is the breather cloth frame draped around the pack. The Mylar top is draped next as in Figure 20, which is followed by the application of the top breather draped over the pack. Figure 21 is the vacuum bag film draped over entire pack.

Patch Build Layer	Regular 9.65 mm (0.38 in.)	Thicker 11.43 mm (0.45 in.)
1	Glass	Glass
2	Bias	Bias
3	Regular	Regular
4	Bias	Bias
5	Regular	Regular
6	Bias	Bias
7	Regular	Regular
8	Bias	Bias
9	Regular	Regular
10	Bias	Bias
11	Regular	Regular
12	Bias	Regular
13	Regular	Regular
14	Bias	Bias
15	Regular	Regular
16	Bias	Regular
17	Regular	Regular
18	Bias	Bias
19	Regular	Regular
20	Bias	Bias
21	Regular	Regular
22	Bias	Bias
23	Glass	Regular
24		Bias
25		Regular
26		Bias
27		Glass

Table 1 - Carbon Fiber Patch Layer Build Schedule
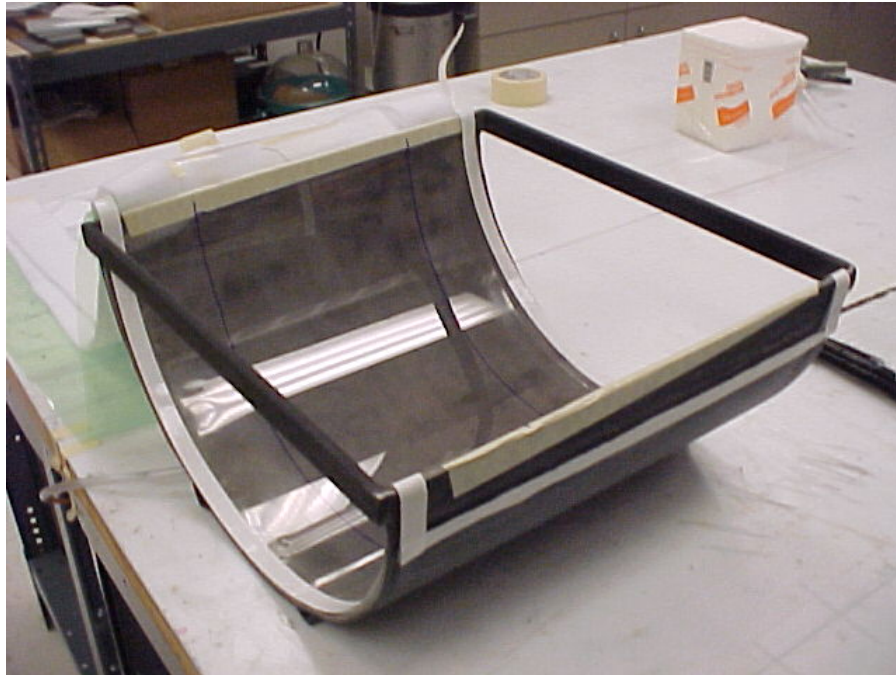
Figure 17 - Mylar-Lined Semi-Circular Mold for Carbon Fiber Patch
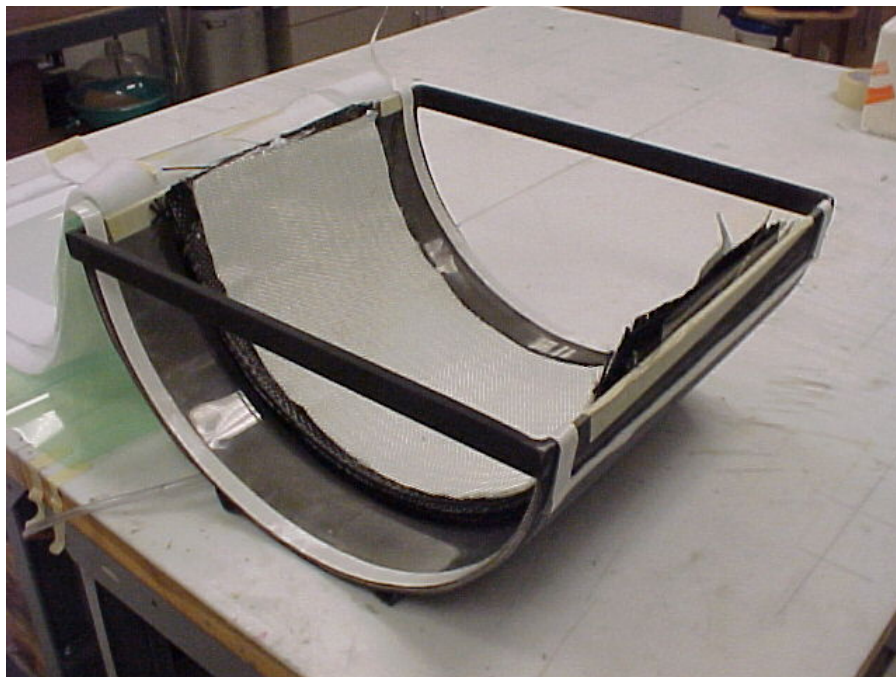
Figure 18 - Dry Pack of Quasi-Isometric Fiber
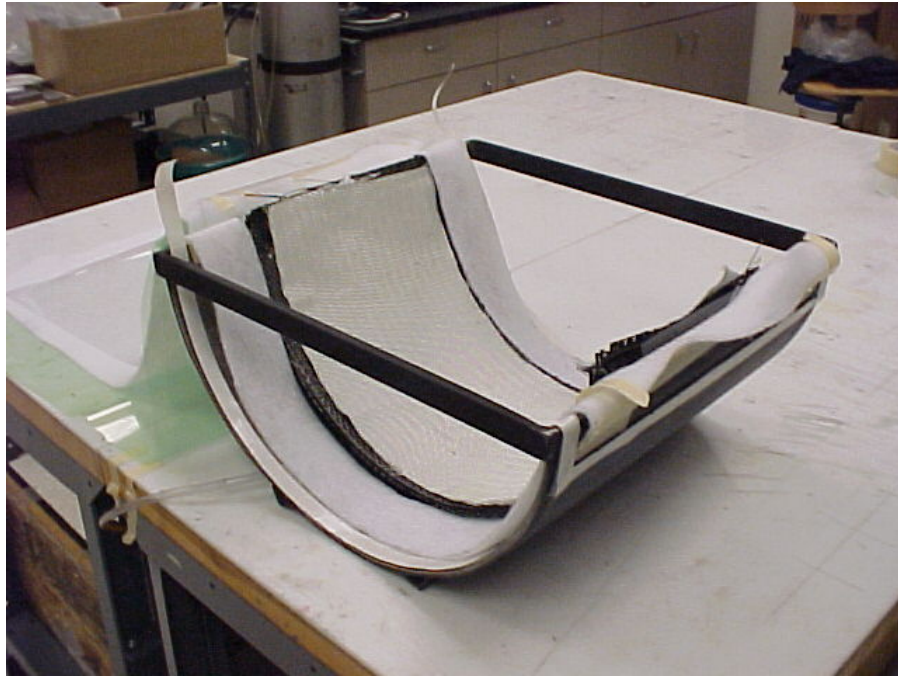
Figure 19 - Breather Cloth Frame Draped Around Pack

Figure 20 - Mylar Top Shown Draped (Top Breather Draped Next Over Pack)

Figure 21 - Vacuum Bag Film Draped Over Entire Pack

FiberGlast 1110 vinylester resin was catalyzed at 1.25% MEKP (9% Oxygen equivalent). The assembly required about 1,600 g (56.43 oz.) of catalyzed resin giving a cup gel time of 75 minutes. Each layer was pre-impregnated with resin as the lay-up proceeded. The hand lay-up was prepared inside the mold with the applied vacuum being maintained until gellation and initial cure was assured (approximately 4 hours). The assembly was then cured overnight. After excising the cured panel, it was trimmed to insertion dimensions. Forced post-cure was not required to maintain dimensions. The calculated fiber volume was between 40% - 45%.

To facilitate patch installation, the outer surface of the patch was grit-blasted using 50 - 80 grit Alumina to remove surface resin (Figure 22). Similarly, the installation area inside the pipe was grit-blasted to a near-white blast with 50 - 80 grit Alumina (Figure 23). After cleaning, a liberal coating of 3M DP460 epoxy adhesive was applied to the internal faying surface and a thin coating was applied to the patch faying surface (Figure 24).

Figure 22 - Completed Repair Patch with Grit-Blasted Outer Diameter
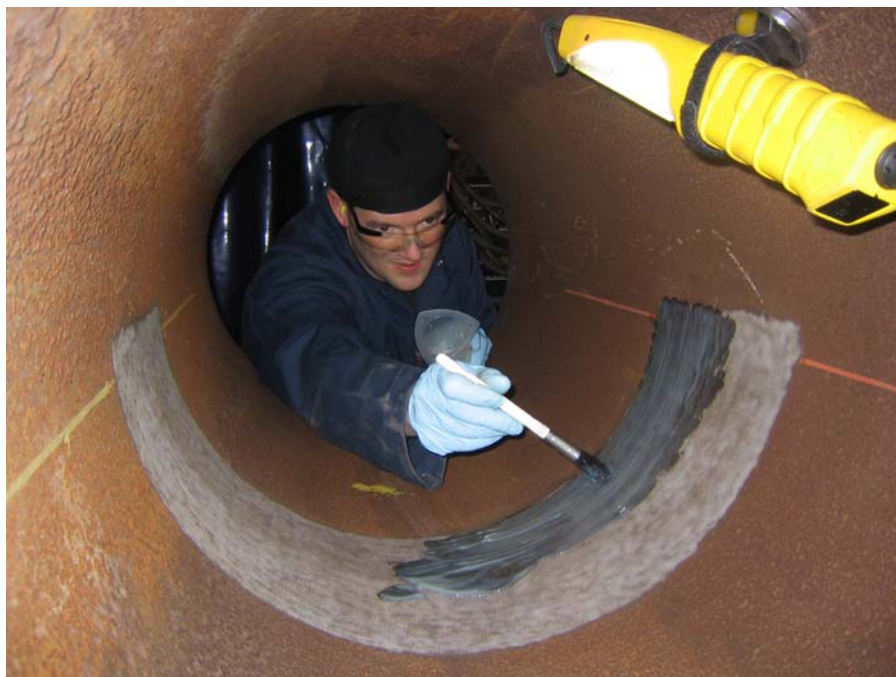
Figure 23 - Application of 3M DP460 Adhesive to Grit-Blasted Inside Diameter of Pipe

Figure 24 - Application of Adhesive to Repair Patch

The patch and pipe section were mated as shown in Figure 25.

Figure 25 - Installation of Repair Patch

Bar clamps were used along the axis of the pipe to hold the patch in place for cure.   Figure 26 shows the adhesive squeeze-out being removed prior to forming a fillet as shown in Figure 27

Figure 26 - Clamping Bars Used to Hold Repair Patch in Place

Figure 27 - Adhesive Fillet Around Repair Patch

Approximately two weeks after the patch cured, the pipe section with the carbon fiber-reinforced liner was hydrostatically tested until failure.

3.2 - Weld Deposition Repair Trials

The project plan includes evaluations of different pipeline repair conditions, such as soil and coating type, on weld deposition repairs. Baseline welding procedures were needed to support these evaluations. Several welding systems were evaluated for internal weld deposition using GMAW and used to develop baseline welding procedures. These evaluations focused on determining whether the systems could make a good internal weld deposit. The pipe axis was fixed in the 5G horizontal position (Figure 28). As welding progressed around the inside diameter, welding position transitioned between flat, vertical, and overhead. The types of envisioned repairs were ring deposits to reinforce a defective weld, spiral deposits to repair an entire pipeline section, and patches to repair local corrosion damage. Weld deposit motion for the first two types would best be achieved using orbital type welding procedures where welding clocks around the circumference. The patch repair could be accomplished using deposit motion that was either orbital or axial. Motion also required the use of torch weaving, a technique that improves out-of-position (i.e., vertical and overhead) weld pool shape. This is common in vertical-up welding to provide an intermediate shelf upon which to progressively build the weld pool deposit. The effects of deposit motion on productivity and quality also required evaluation for this application. With the different welding systems, the preferred metal transfer mode for GMAW was short-circuiting transfer. This mode assures drop transfer in all welding positions. Open arc droplet transfer that is provided by spray, pulse spray, and globular transfer are not suitable for spiral overhead welding where gravity promotes spatter instead of metal transfer.

Centerline
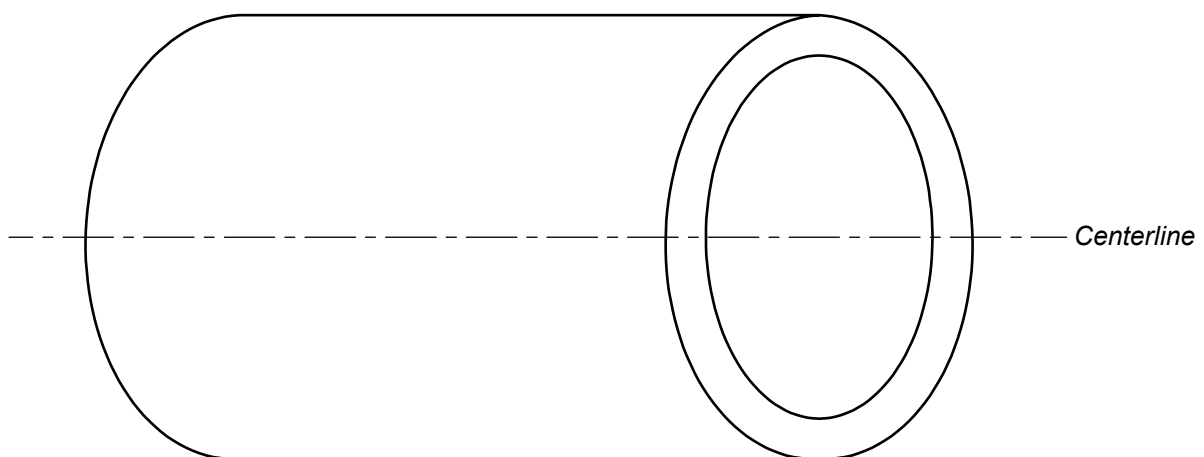
Figure 28 - Pipe in the 5G Horizontal and Fixed Position

The following welding systems were evaluated for internal repair of pipelines:

- Internal bore cladding system (Bortech)

- 6-axis robot capable of complex motion control (OTC Daihen)

- Orbital welding tractor configured for inside welding (Magnatech Pipeliner)

Each system had motion control limitations and individually would not be appropriate candidates for an internal repair welding system. The internal bore cladding system manufactured by Bortech (Figure 29 and Figure 30) was designed for spiral cladding the inside of pipe that is preferably in the vertical position.

Figure 29 - Bortech Motion Mechanism for Continuous Spiral Deposition

Figure 30 - Bortech Torch and Torch Height Control

The Bortech system has simple controls for operating constant voltage (CV) power supplies (Figure 31). This includes the ability to set wire feed speed, voltage, step size (for the spiral motion), and rotation speed (i.e., travel speed). The system is very affordable as it uses simple motors for motion. When positioned inside a horizontal pipe, the rotation drive suffered from significant backlash. Conversations with the supplier led to the purchase and installation of a counterbalance weight that was used to balance the weight of the opposing torch.

Figure 31 - Bortech Controller

Preliminary weld trials with the Bortech system had marginal results. Only stringer beads were successfully deposited using short-circuit transfer in the spiral clad mode. Travel speeds of 3.81 mpm (150 ipm) to 4.45 mpm (175 ipm) were used with an 0.89 mm (0.035 in.) diameter ER70S-6 filler metal (i.e., electrode). With stringer beads, the deposition rate was low since only narrow beads could be deposited. The bead shape suffered the most in the overhead position when starting downhill. Weaving was required to improve weld bead profile thus allowing higher deposition rates and improved fusion. The off-the-shelf system did not permit oscillation, but could if adapted with modern controls. In principle, this type of mechanism would be suitable for an internal repair system. Here, anti-backlash servo-motors and gears, and programmable controls would be required to improve the system. Similarly, an additional motor drive that permits control of torch and work angle would also be required to cope with all the possible repair scenarios to optimize bead shape.

Based on the results experienced with the Bortech system, it was decided to develop preliminary welding procedures using a robotic GMAW system. A 6-axis coordinated motion robot (Figure 32) permitted the application of weave beads for spiral cladding or stringer beads in either direction. An observed limitation was the fact that the system did not have a welding torch current commutater to permit continuous spiral welding.

Figure 32 - OTC Robot Set-Up for Internal Welding

The standard robot welding torch (Figure 33) could only be used for half a revolution, then it had to be unwound to complete the remainder of each deposit ring. This limitation was acceptable for parameter development since the focus was the welding parameters not high duty cycle welding. The robot was interfaced to an advanced short-circuit power supply, the Kobelco PC-350.
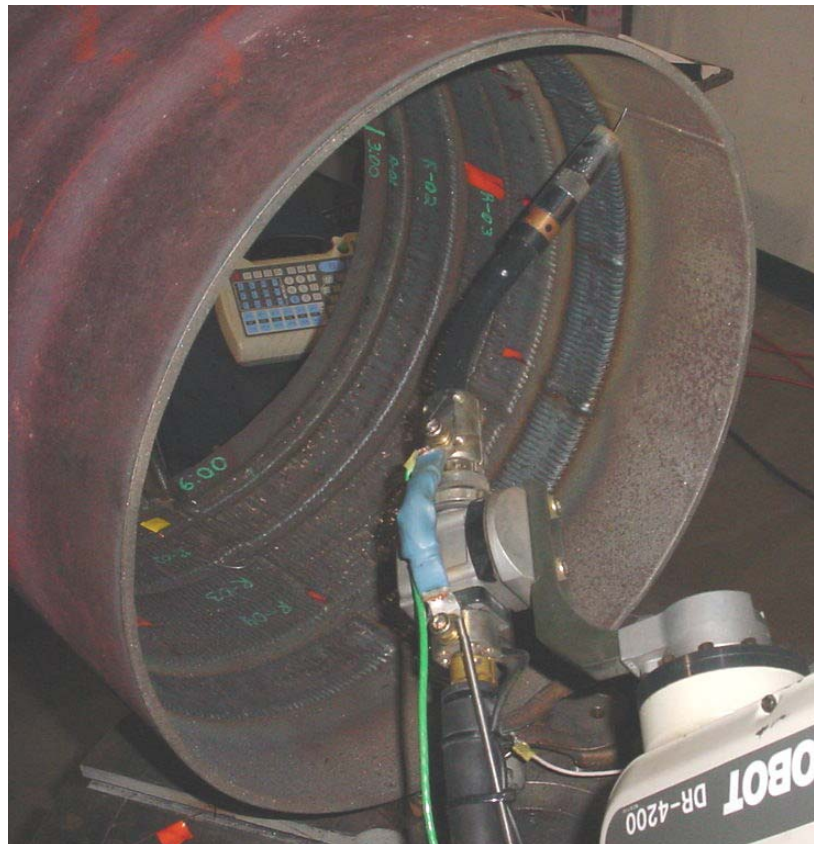
Figure 33 - OTC Robot Arm and Torch

The Kobelco PC-350 power supply (Figure 34) uses fuzzy logic pulse waveforms to minimize spatter during metal transfer and permits the application of variable polarity waveforms. Variable polarity combines the rapid, low heat input, melting of negatively charged electrode with the metal transfer stability of electrode positive. Until 1988, all commercial GMAW systems used positively charged electrodes for constant voltage and pulse power supplies. The PC-350 is more advanced than standard variable polarity power supplies, as it uses a fuzzy logic short-circuit anticipation control. On comparable applications that require low heat input, the PC-350 has shown productivity improvements compared to standard short-circuit. This power supply is equipped with waveform algorithms pre-programmed for steel using either 100% Carbon Dioxide shielding gas or an Argon - Carbon Dioxide shielding gas mixture for both

0.8 mm (0.035 in.) or 1.2 mm (0.045 in) diameter electrodes. The waveform was simply modified by changing the electrode negative ratio on the pendant. Arc length and heat input is changed by an arc length knob on the pendant, which varies the pre-programmed pulse frequency.

Figure 34 - Kobelco PC-350 Variable Polarity Fuzzy Logic Power Supply

The OTC robot welding system was used to develop preliminary repair welding procedures with the intent that they would be transferred to a different system for pipeline repair demonstrations. A range of orbital (ring motion) weave parameters were developed to establish an operating window, deposit quality, and deposition rate. Preliminary tests were also performed to evaluate bead overlap and tie-in parameters that would be required to make high quality repairs. All the welding tests were performed with a 95% Argon - 5% Carbon Dioxide shielding gas mixture using an 0.89 mm (0.035 in.) diameter ER70S-6 electrode.

Several years ago, PG&E purchased a welding tractor (Figure 35) from Magnatech for internal weld repair procedure development. This system was sent to EWI for this project so it could be used for pipeline repair testing and demonstrations, since this equipment is portable where the robot welding system is not portable.
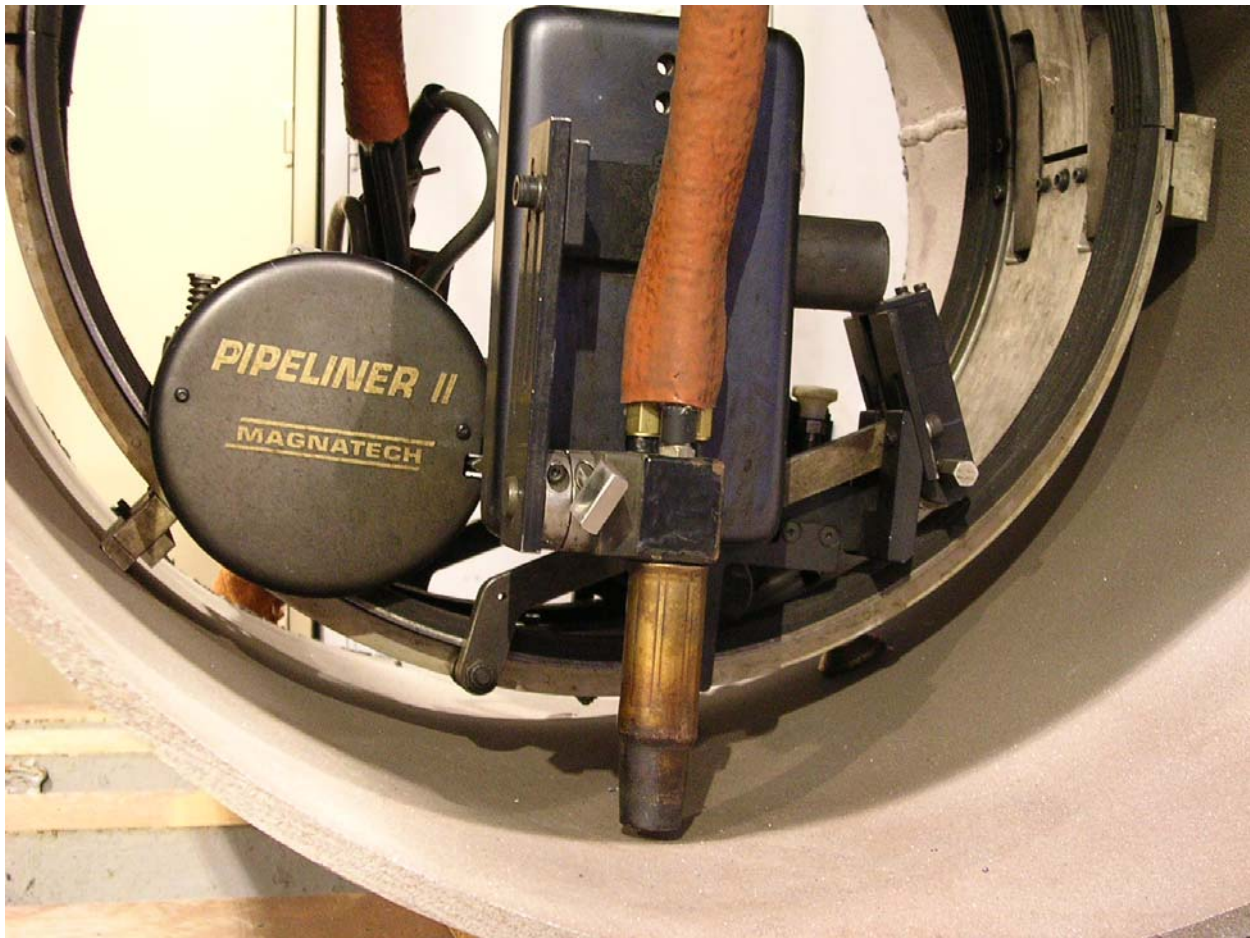
Figure 35 - Magnatech ID Welding Tractor Capable of Spiral & Ring Motion with Oscillation

The Magnatech welding tractor has orbital motion with controls (Figure 36) for torch oscillation. The system is limited to a finite number of revolutions that can be made before cables need to be unwound. The controls are analog and do not have high accuracy, however, they are sufficient for preliminary parameter development and demonstration welding. Programmable controls would be required for an internal repair welding system using a Magnatech tractor. In addition, numerous mechanical changes would be required to accommodate a range of pipeline diameter sizes.

Figure 36 - Magnatech Control Pendant Showing Control Parameters

The Magnatech tractor was interfaced to a Panasonic AE 350 power supply (Figure 37). This power supply provides pulse waveforms and can be operated in a short-circuit mode where artificial intelligence is used to minimize spatter. The current pulsing and short circuiting helps lower heat input and improve deposition rate in out-of-position welds. Pre-programmed current waveforms are provided by algorithms for steel electrodes, and many other materials.

Figure 37 - Panasonic AE 350 Power Supply with Pulse Short-Circuit Metal Transfer Control

PG&E bought the Magnatech Pipeliner system specifically to repair weld 559 mm (22 in.) diameter pipe. In order to use the PG&E system for this project, Panhandle Eastern supplied approximately 12.19 m (40 ft.) of asphalt covered, 559 mm (22 in.) diameter pipe that was made in the 1930s. Additional lengths of 508 mm (20 in.) diameter pipe of similar vintage were already in the EWI material inventory.

Successful procedures were developed on the Magnatech Pipeliner system to determine the feasibility of making welds on the inside diameter (ID) to replace metal loss on the outside diameter (OD) due to corrosion damage. Also using the Magnatech system, the effect of methane in the welding environment was evaluated with respect to the integrity of resultant weld quality as the amount of methane was varied in the shielding gas.

The simulated corrosion in the pipe was introduced by milling a slot into a 559 mm (22 in.) OD pipe with a wall thickness of 7.9 mm (0.312 in.) using the set-up as shown in Figure 38. The dimensions of the corrosion damage are shown in Figure 39; finished simulated damage is found in Figure 40; and a magnified view of the damage is located in Figure 41.

Figure 38 - Milling Machine Set-Up Used to Simulate Corrosion on Pipe Sections
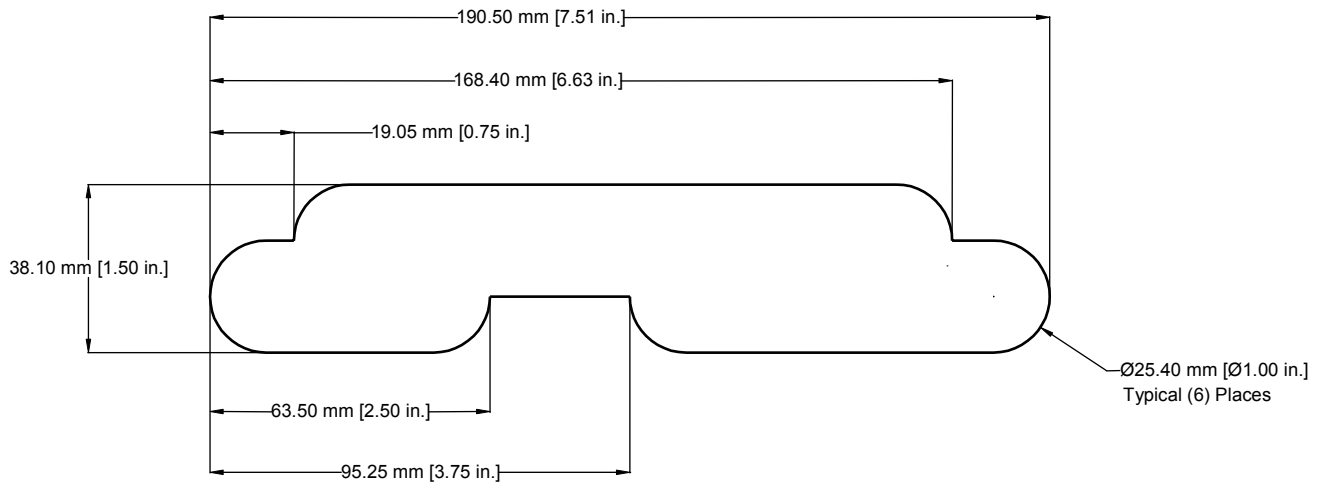
Figure 39 - Dimensions of Simulated Corrosion on 558.80 mm (22 in.) Pipe

190.50 mm [7.51 in.]

168.40 mm [6.63 in.]

19.05 mm [0.75 in.]

38.10 mm [1.50 in.]

Ø25.40 mm [Ø1.00 in.]
Typical (6) Places

63.50 mm [2.50 in.]

95.25 mm [3.75 in.]

Figure 40 - Simulated Corrosion on 558.80 mm (22 in.) Pipe

41633R47.pdf

Figure 41 - Magnified View of Simulated Corrosion on 558.80 mm (22 in.) Pipe

Using the RSTRENG software, the burst pressure corresponding to 100% of the SMYS of the pipe and the burst pressure after milling the simulated corrosion were both calculated (see Table 2).

Pipe Outside Diameter	558.80 mm (22 in.)
Wall Thickness	7.92 mm (0.312 in.)
Pipe Material	API 5L-Grade B
Type of Damage	Simulated Corrosion Defect
Damage Length	190.50 mm (7.5 in.)
Damage Depth	3.96 mm (0.156 in.)
Damage as % of Wall Thickness	50%
RSTRENG-predicted burst pressure for pipe with damage	5.15 MPa (747 psi)
RSTRENG-predicted burst pressure compared to pressure at 100% SMYS	75%

Table 2 - Burst Pressures for Weld Deposition Repairs on 558.8 mm (22 in.) Diameter Pipe

For the internal weld deposition trials, a shielding gas mixture of 95% Argon (Ar) - 5% Carbon Dioxide (CO_2) was used in conjunction with the welding process parameters shown in Table 3and Table 4.

Layer	Pass	Wire Feed Speed (mpm)	Current (amps)	Volts	Length (mm)	Time (sec)	Travel Speed (mpm)	Heat Input (kJ/mm)
1	1	5.44	100	19.9	158.750	165	0.058	2.07
	2	5.51	97	19.8	165.100	175	0.057	2.04
	3	5.46	96	19.9	171.450	173	0.059	1.93
	4	5.49	98	19.8	165.100	173	0.057	2.03
	5	5.46	98	19.8	168.275	185	0.055	2.13
	6	5.46	99	20.0	171.450	191	0.054	2.21
	7	5.38	98	19.9	171.450	192	0.054	2.18
	8	5.46	99	19.8	174.625	200	0.052	2.24
	9	5.44	98	19.8	171.450	200	0.051	2.27
	10	5.38	98	19.5	174.625	197	0.053	2.16
	11	5.46	100	19.6	174.625	192	0.055	2.16
2	1	5.49	96	19.9	155.575	179	0.052	2.20
	2	5.41	98	19.8	165.100	179	0.055	2.11
	3	5.38	99	19.9	155.575	171	0.055	2.17
	4	5.51	98	19.8	161.925	187	0.052	2.24
	5	5.46	104	19.6	160.274	176	0.055	2.24
	6	5.44	101	19.8	165.100	189	0.052	2.29
	7	5.46	98	19.8	165.100	189	0.052	2.22
	8	5.46	96	19.9	163.576	199	0.049	2.32
	9	5.46	100	19.8	166.624	204	0.049	2.42
	10	5.49	101	19.8	169.545	205	0.050	2.42

Table 3 - Metric Unit Welding Parameters for Internal Weld Deposition Repair

Weld Layer	Pass	Wire Feed Speed (ipm)	Current (amps)	Volts	Length (in)	Time (sec)	Travel Speed (ipm)	Heat Input (kJ/in)
1	1	214	100	19.9	6.25	165	2.27	52.5
	2	217	97	19.8	6.50	175	2.23	51.7
	3	215	96	19.9	6.75	173	2.34	49.0
	4	216	98	19.8	6.50	173	2.26	51.6
	5	215	98	19.8	6.63	185	2.15	54.2
	6	215	99	20.0	6.75	191	2.12	56.0
	7	212	98	19.9	6.75	192	2.11	55.4
	8	215	99	19.8	6.88	200	2.06	57.0
	9	214	98	19.8	6.75	200	2.02	57.6
	10	212	98	19.5	6.88	197	2.09	54.8
	11	215	100	19.6	6.88	192	2.15	54.7
2	1	216	96	19.9	6.13	179	2.06	55.8
	2	213	98	19.8	6.50	179	2.18	53.5
	3	212	99	19.9	6.13	171	2.15	55.1
	4	217	98	19.8	6.38	187	2.04	57.0
	5	215	104	19.6	6.31	176	2.15	57.0
	6	214	101	19.8	6.50	189	2.06	58.1
	7	215	98	19.8	6.50	189	2.06	56.4
	8	215	96	19.9	6.44	199	1.94	59.0
	9	215	100	19.8	6.56	204	1.93	61.5
	10	216	101	19.8	6.68	205	1.95	61.5

Table 4 - U.S. Customary Unit Welding Parameters for Internal Weld Deposition Repair

The dirt box in Figure 42 was used to simulate in-service welding conditions and cooling rates for weld deposition repair evaluation trials.

Figure 42 - Dirt Box for Weld Deposition Repair

The pipe section with the dirt box was rotated as shown in Figure 43 to facilitate welding on the inside of the pipe section from the 6:00 position where the weld passes were initiated to the 9:00 position where the weld passes were terminated.

Figure 43 - Orientation of Pipe Section with Dirt Box for Weld Deposition Repair

An outline of the simulated corrosion was made on the ID of the pipe (Figure 44) to assure the deposited weld metal completely covered the area of simulated corrosion on the inside of the pipe.
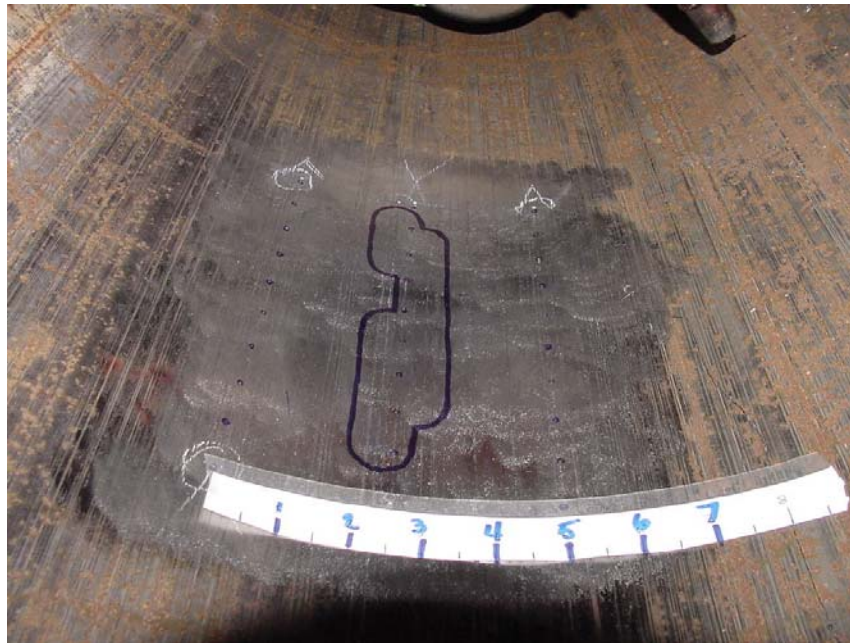
Figure 44 - Outline of Simulated Corrosion on Inside Diameter of Pipe Section

The first pass of the first layer of the ID weld repair is shown in Figure 45.
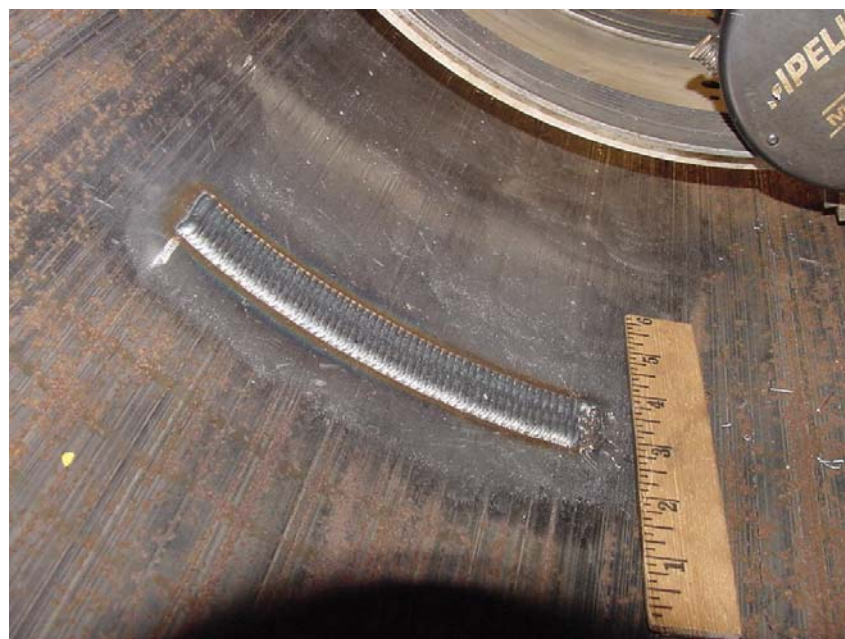
Figure 45 - First Pass of First Layer of Deposited Weld Metal on Inside Pipe Diameter

For the first layer of weld deposition, each subsequent weld pass overlapped the previous weld pass by 1.5 mm (0.06 in.). The second pass of the first layer of the ID weld repair is shown in Figure 46.
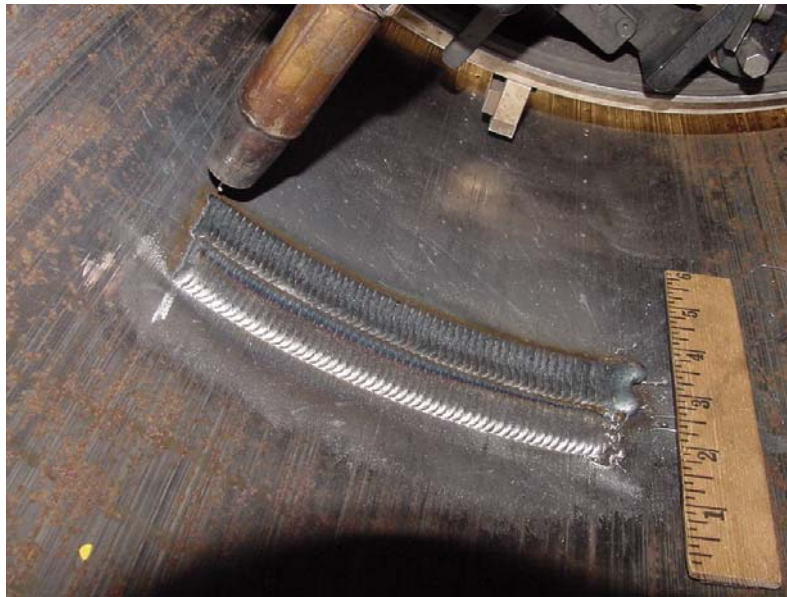
Figure 46 - Second Pass of First Layer of Deposited Weld Metal on Inside Pipe Diameter

During execution of the third pass of the first layer of deposited weld metal, a small defect was created as indicated in the yellow circle in Figure 47. The defect was repaired with an autogenous (i.e., with no filler metal) gas tungsten arc weld (GTAW).
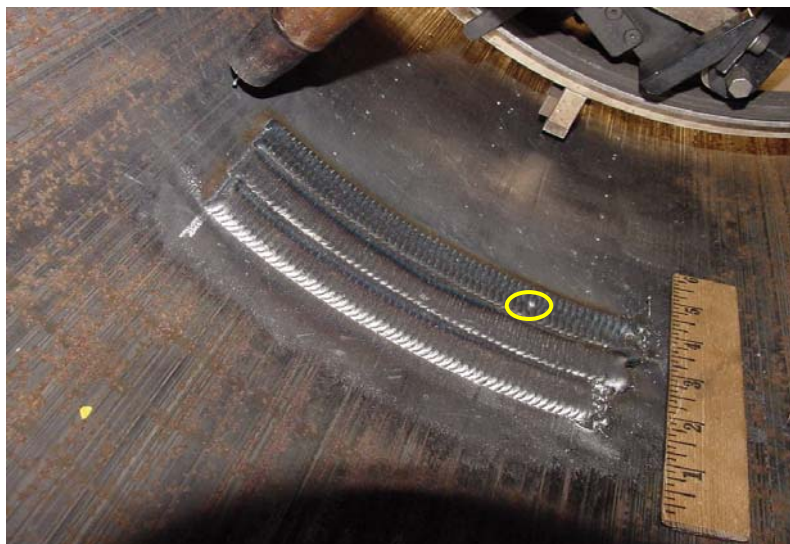
Figure 47 - Third Pass of First Layer of Deposited Weld Metal on Inside Pipe Diameter

The finished first layer of the deposited weld metal repair is shown in Figure 48. The axial length of the deposited layer exceeded the simulated corrosion by more than 25.4 mm (1.0 in.), which is three times the pipe wall thickness (the weld deposit should exceed the corrosion area by at least one wall thickness).

Figure 48 - Finished First Layer of Deposited Weld Metal on Inside Pipe Diameter

First pass of the second layer is shown in Figure 49. The second layer passes were centered over the weld toes of the previous layer.

Figure 49 - First Pass of Second Layer of Deposited Weld Metal on Inside Pipe Diameter

Completed second layer is shown in Figure 50.

Figure 50 - Finished Second Layer of Deposited Weld Metal on Inside Pipe Diameter

For the methane evaluation study, shielding gas was supplied by two independent gas bottles: one bottle contained a mixture of 95% Ar - 5% CO_2; the other bottle contained a mixture of 10% methane with a balance of 95% Ar - 5% CO_2. The amount of methane was raised by increasing the flow rate on the flow meter of the bottle containing methane. Linear travel speeds of the welds were not recorded as it was held constant for the preparation of all weld specimens. Methane welding process parameters are found in Table 5.

| Weld ID | Shielding Gas Flow Rate | | | | Voltage (volts) | Current (amps) | Wire Feed Speed | |
| | 95% Ar + 5% CO_2 | | 10% Methane + 4.5% CO_2 + 85.5% Ar | | | | | |
	(m³/hr)	(ft³/hr)	(m³/hr)	(ft³/hr)			(mpm)	(ipm)
325-2	1.41	50	0.00	0	23.4	111	5.36	211
325-6	1.22	43	0.20	7	23.4	104	5.23	206
325-3	1.13	40	0.28	10	23.3	108	5.28	208
325-8	0.99	35	0.28	10	23.2	101	5.26	207
325-4	0.99	35	0.42	15	23.4	99	5.08	200
325-9	0.85	30	0.42	15	23.1	97	5.56	219
325-5	0.85	30	0.57	20	23.1	96	5.41	213

Table 5 - Welding Process Parameters for Weld Deposition Repairs in Methane

3.3 - Baseline Pipe Material Performance

Because of the large discrepancies in the predicted hydrostatic burst pressures and the actual burst pressures, additional physical testing was performed. Tensile testing was conducted on 508 mm (20 in.) and 558.8 mm (22 in.) pipe material. Four additional hydrostatic pressure tests were also conducted to establish baseline performance data for un-repaired pipe sections in the virgin condition (i.e., undamaged) and with un-repaired simulated corrosion damage.

Simulated corrosion damage (similar to that found in Figure 39 and Figure 41) was introduced into one section of 558.8 mm (22 in.) diameter by 7.93 mm (0.312 in.) thick API 5L Grade B pipe and into one section of 508 mm (20 in.) diameter by 6.4 mm (0.25 in.) wall API 5LX-52 pipe. No repair processes were applied to either pipe section with simulated damage. Both pipe sections were assembled as shown in Figure 14 to prepare for burst testing. Two pipe sections in the virgin condition, one section of 558.8 mm (22 in.) diameter by 7.93 mm (0.312 in.) thick API 5L Grade B pipe and one section of 508 mm (20 in.) diameter by 6.4 mm (0.25 in.) wall API 5LX-52 pipe, were assembled as shown in Figure 14 to prepare for burst testing. All four un-repaired pipe sections were then hydrostatically tested until failure.

3.4 - Simulation and Analysis of Potential Repairs

The composite liner requirements were determined from the assumed values for an economical carbon fiber reinforcement with a vinylester resin system. The objective was to define realistic combinations of composite material and thickness for use in liner systems for internal repair of natural gas transmission pipelines.

Two simple cases were investigated. The first case is one in which the entire steel pipe has been lost to external corrosion, leaving only the liner to carry the external stress. The second case is one in which shear failure occurs in the matrix material between the layers of fibers. EWI chose an initial pipeline size in the middle of the commonly used range for transmission pipelines: a 508 mm (20 in.) outside diameter pipe with a 6.35 mm (0.25 in.) wall thickness made from X-65 pipe material. For this situation, the additional liner material could not be so thick as to prevent subsequent examinations of the adjacent steel pipeline by internal inspection devices and was limited the thickness of the simulated liner to less than 12.7 mm (0.5 in.).

4.0 - RESULTS AND DISCUSSION

This report is a review and evaluation of internal pipeline repair trials during the first twenty-one months of work for a project sponsored by the U.S. Department of Energy (DOE) National Energy Technology Laboratory (NETL) to develop internal repair technology for gas transmission pipelines. In order to thoroughly investigate repair technology, this project brings together a combination of partners that have a proven track record in developing pipeline repair technology. The project team consists of Edison Welding Institute (EWI), a full-service provider of materials joining engineering services; Pacific Gas & Electric (PG&E), a pipeline company that has a current need for the technology; and the Pipeline Research Council International (PRCI), an international consortium of pipeline companies, to provide project oversight and direction. EWI is the lead organization performing this Award for NETL in Morgantown, West Virginia.

4.1 - Development of Internal Repair Test Program

Experimental work evaluated the potential repair methods of fiber-reinforced composite repairs and weld deposition repairs.

Fiber-Reinforced Liner Repairs

A preliminary test program of small-scale experiments for glass fiber-reinforced composite repairs were conducted in order to take advantage of existing tooling for the RolaTube product. API 5L Grade B pipe sections with a 114.3 mm (4.5 in.) diameter and a 4 mm (0.156 in.) thick wall were used with a 2.85 mm
(0.11 in.) thick glass polypropylene liner.

Following the installation of end caps, all four pipe sections were hydrostatically pressurized to failure. All four pipe sections failed in the areas of simulated corrosion damage. The two pipes with long shallow damage representative of general corrosion resulted in ruptures (Figure 51 and Figure 52) and the two pipes with short, deep damage representative of a deep isolated corrosion pit developed leaks (Figure 53 and Figure 54). The hydrostatic testing results are shown in Table 6.

Figure 51 - Pipe Section with Long, Shallow Simulated Corrosion Damage – Without Liner - Following Hydrostatic Pressure Test

Figure 52 - Pipe Section with Long, Shallow Simulated Corrosion Damage – With Liner – Following Hydrostatic Pressure Test
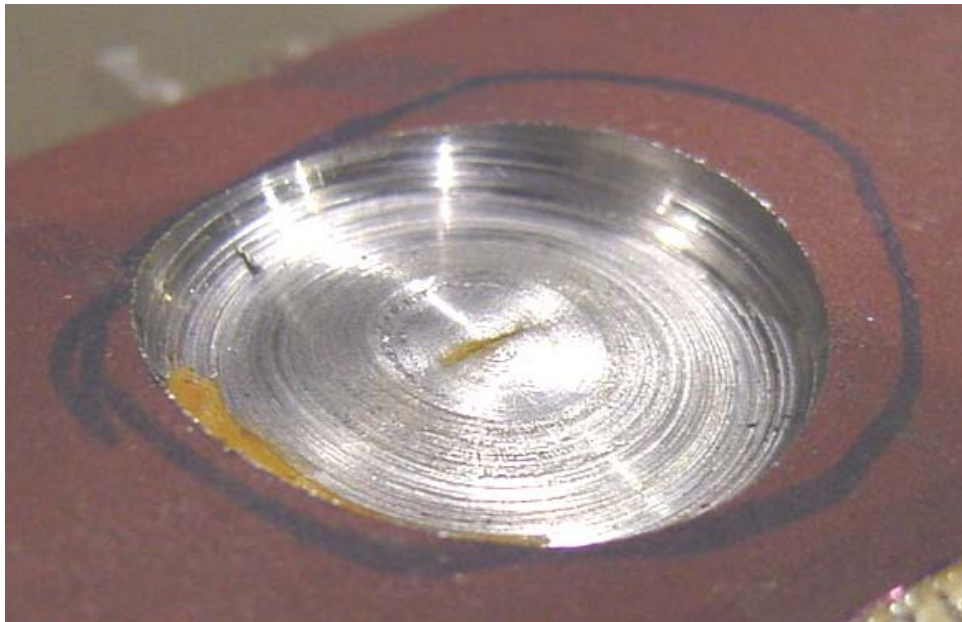
**Figure 53 - Pipe Section with Short, Deep Simulated Corrosion Damage – Without Liner –
Following Hydrostatic Pressure Test**
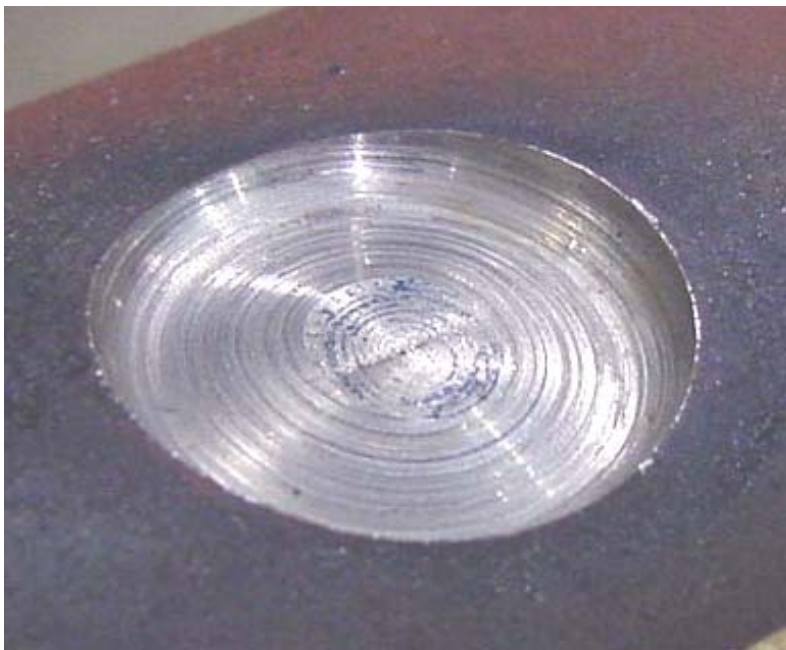
**Figure 54 - Pipe Section with Short, Deep Simulated Corrosion Damage – With Liner –
Following Hydrostatic Pressure Test**

Simulated Corrosion Damage	Liner	Hydrostatic Failure Pressure MPa (psi)	Failure Mode/Location
Long, Shallow	No	23.6 (3,431)	Rupture in simulated corrosion damage
Long, Shallow	Yes	23.9 (3,472)	Rupture in simulated corrosion damage
Short, Deep	No	25.8 (3,750)	Leak in simulated corrosion damage
Short, Deep	Yes	27.7 (4,031)	Leak in simulated corrosion damage

Table 6 - Hydrostatic Pressure Testing Results

The failure pressures for the pipes with the liners were only marginally greater than the pipes without the liners (i.e., 23.9 MPa (3,472 psi) vs. 23.6 MPa (3,431 psi) for the pipe specimens containing long shallow damage and 27.7 MPa (4,031 psi) vs. 25.8 MPa (3,750 psi) for the pipe specimens containing short, deep damage), indicating that the glass fiber-reinforced liners were generally ineffective at restoring the pressure containing capabilities of the pipes.

A postmortem analysis of the first four hydrostatic burst tests in pipe sections with simulated corrosion was conducted. So as not to damage the liner, water jet cutting was used to section the pipe sample containing the round-bottom longitudinal slot with the liner installed. The results indicate that the liner did rupture (Figure 55 and Figure 56), thus disbonding was not an issue.

Figure 55 - Water-Jet Cut Section through Pipe Sample Containing Round-Bottom Longitudinal Slot with Liner Installed

Figure 56 - Pipe Sample Containing Round-Bottom Longitudinal Slot Showing Rupture of Liner Material

Postmortem test results also indicate that the difference in modulus of elasticity between the steel and the liner material prevents the liner from carrying its share of the load. The modulus of elasticity for steel is approximately 206.8 GPa (30 x 10^6 psi). Tensile testing was carried out to determine the modulus of elasticity for the glass/polypropylene liner material that was used (Table 7 and Figure 57). The mean value for the modulus of elasticity for the liner material was measured to be approximately 15.2 GPa (2.2 x 10^6 psi). Because the glass fiber-reinforced liner material has a significantly lower modulus of elasticity than the steel pipe, as pressure in the lined pipe increases, the stiffness of the steel prevents the composite liner material from experiencing enough strain to share any significant portion of the load.

	Stress at Break MPa (ksi)	Strain at Break (%)	1% Secant Modulus MPa (ksi)
Trial 1	486.6 (70.58)	4.34	15,123.4 (2,193.394)
Trial 2	557.6 (80.88)	4.21	17,166.7 (2,489.741)
Trial 3	492.0 (71.36)	5.21	17,316.5 (2,511.472)
Trial 4	371.5 (53.89)	5.02	14,103.5 (2,045.482)
Trial 5	460.9 (66.85)	4.56	14,347.9 (2,080.924)
Trial 6	154.7 (22.45)	4.51	15,191.0 (2,203.205)
Mean	420.6 (61.00)	4.64	15,541.5 (2,254.036)
S. D.	143.4 (20.81)	0.39	1,384.3 (200.776)
C. V.	235.1 (34.11)	8.45	61.4 (8.907)
Minimum	154.7 (22.45)	4.21	14,103.5 (2,045.482)
Maximum	557.6 (80.88)	5.21	17,316.5 (2,511.472)
Range	402.8 (58.43)	1.00	3,213.0 (465.990)

Table 7 - Tensile Testing Results for Glass/Polypropylene Liner Material
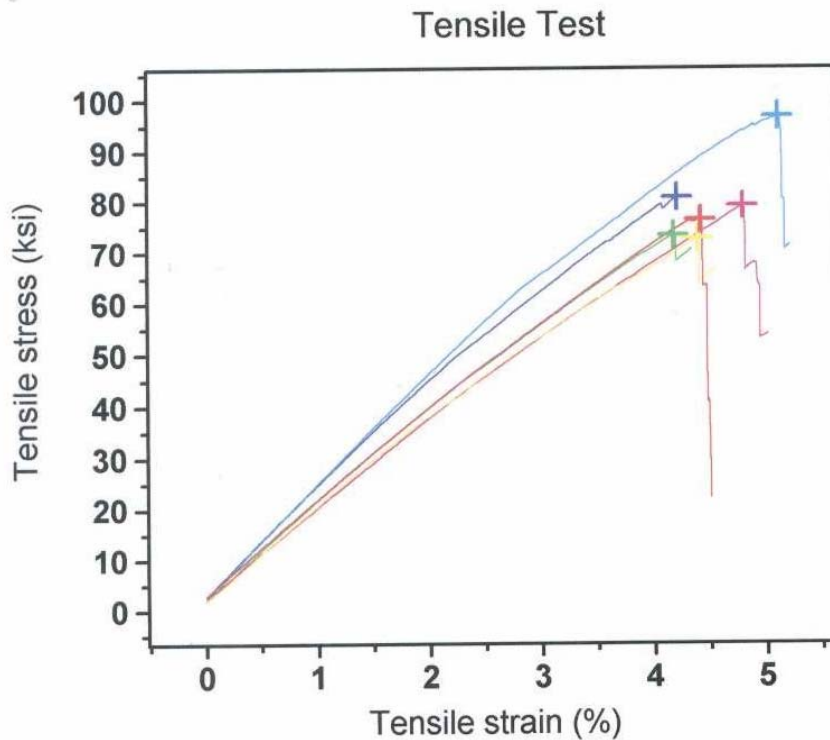
Figure 57 - Tensile Testing Results for Glass/Polypropylene Liner Material

It is anticipated that a liner material with a modulus of elasticity on the order of 95% of that for steel will be required for effective reinforcement of steel pipelines that have been weakened by wall loss defects (e.g., by eternal corrosion). A liner material with a modulus of elasticity that is just less than that of steel (i.e., on the order of 95%) would allow the liner to carry its share of the load without putting the interface between the liner and the steel pipe in tension. If the modulus of elasticity for the liner material were greater than that of the steel pipe, as pressure in the pipe increases, the stiffness of the liner would prevent it from expanding with the steel pipe, putting the weak adhesively-bonded interface in tension. If the adhesive layer between the pipe and the sleeve were to be broken, this would allow pressure into the annular space between the pipe and liner, allowing the pressure to act upon the defect-weakened area and rendering the liner useless.

Weld Deposition Repairs

A preliminary test program for deposited weld metal repairs was developed. This test program initially focused on developing GMAW parameters necessary to complete an internal circumferential weld deposition repair.

Arc welding processes offer a viable repair method that can be applied from the inside of a gas transmission pipeline. There are several arc welding processes that can be operated remotely. Based on the survey and assessment of candidate arc welding processes, the GMAW process was the most likely choice for this application. It offers a good combination of simplicity, high productivity, robustness, and quality that are required for this welding repair application. Arc welding processes are routinely used to externally repair pipelines. However, repair from the inside offers new challenges for process control since welding will need to be performed remotely. In addition, since the intent is to leave an unexcavated pipeline in the ground, there are several variables that will affect the welding process and quality. Soil conditions have the potential to influence heat removal during welding thereby altering the fusion characteristics, welding cooling rate, and mechanical properties. The effects of welding on the external coating used to protect against corrosion will need to be evaluated to assure future pipeline integrity. Finally, if welding was performed in-service, the pressure and flow rate of the gas will have a strong effect on the equipment design of the welding process. New process equipment technology will be required to shield the welding process from methane contamination and cope with higher gas pressures. A significant deliverable will be the development of an equipment specification defining all the functional requirements for an internal repair welding system.

Preliminary welding procedures were developed using the 6-axis robot. The objective of these tests was to establish deposit layer parameters that could be used to make ring, spiral or patch repairs. Since the objective for these repairs is to reinforce the wall thickness, the bead shape criteria was to make flat deposits. If a large area needed repaired, multiple weld beads would

be tied to each other. Here, bead overlap parameters need to be developed to optimize the uniformity of the entire repair deposit area. In many ways, the parameters that were developed are similar to cladding procedures. The ideal weld bead shape would have uniform thickness across the weld section except near the weld toes, which should taper smoothly into the base material (Figure 58). Smooth toes promote good tie-ins with subsequent weld beads. The fusion boundary should be uniform and free from defects.

Weld Bead

Weld Toe

Base Metal
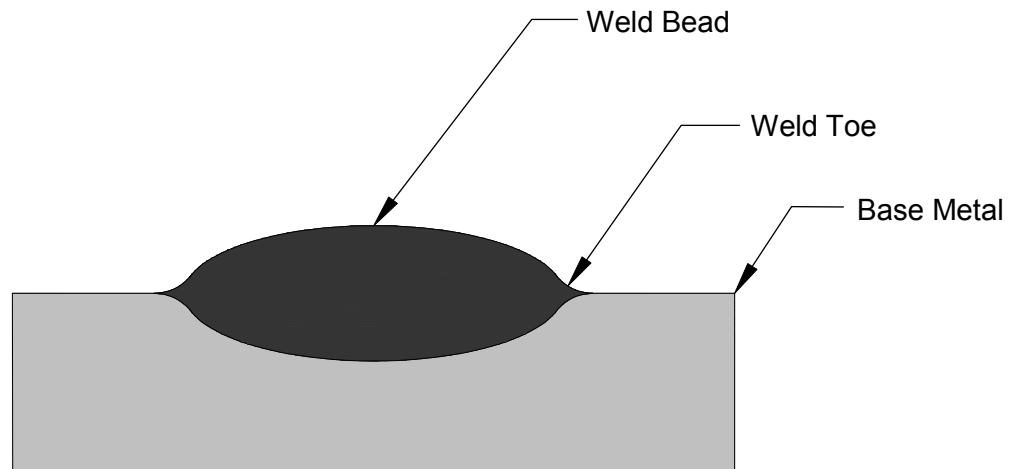
Figure 58 - Weld Bead Shape Diagram

Using the robot welding system, ring welding procedures using weaving were developed for several bead widths (Figure 59). This figure shows the location were the first half of the ring was stopped and the second half was started in the overhead position. This was not an ideal stop-start location but was required with the robot to manage the welding cables.   If start-stops were required to complete a repair, it would be preferred to have them positioned at a different location around the circumference, ideally in the flat position.   Tie-in parameters will need to be optimized for each possible starting position once preferred bead shape weaving parameters are selected. A true orbital bore welding machine, like the Bortech, would have a current and shielding gas commutation system to provide infinite rotations without cable problems thereby minimizing stop-starts.
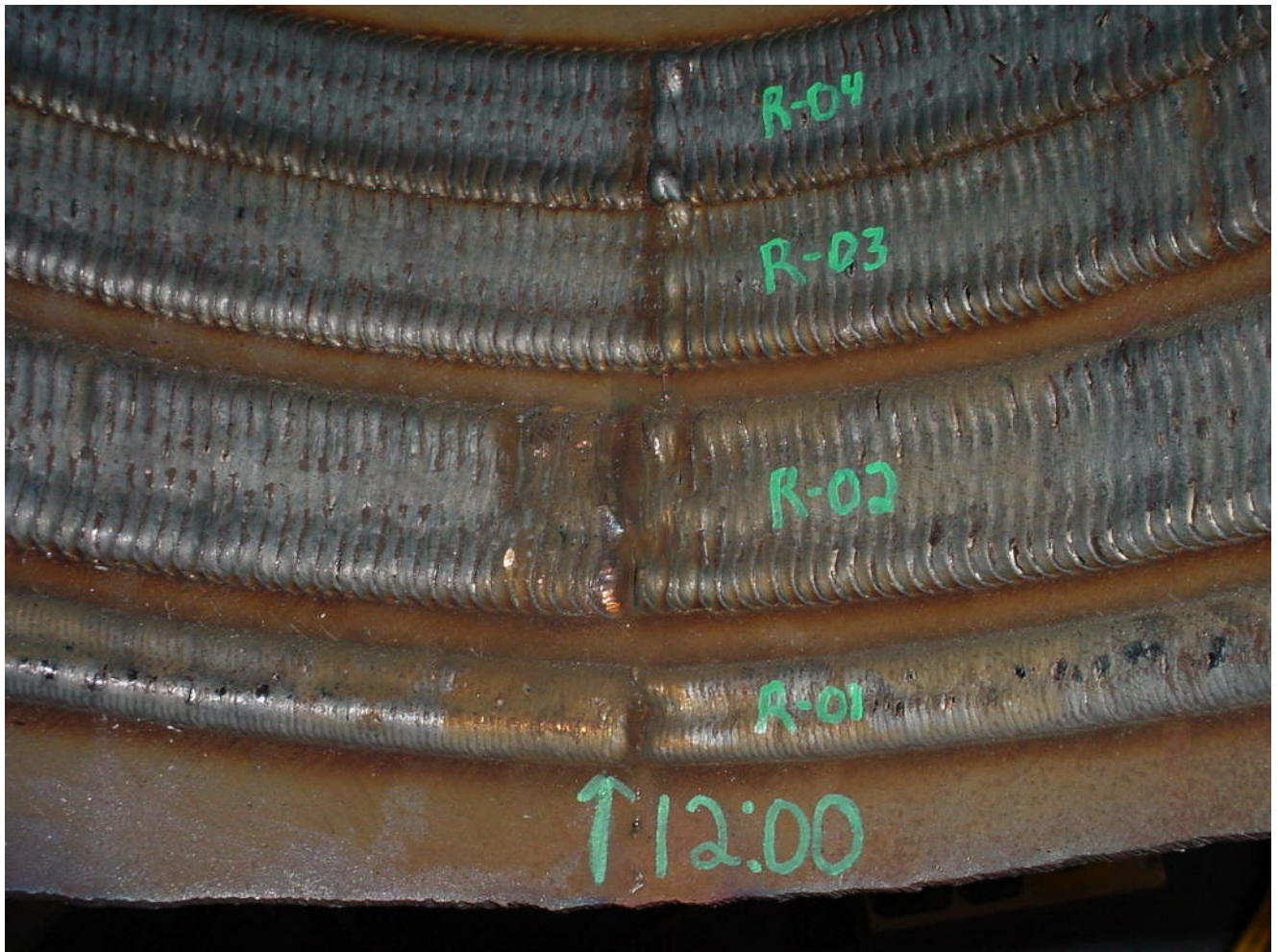
Figure 59 - Tests R-01 through R-04 at 12:00 (Note the Poor Tie-Ins for R-01 through R-03)

When welding is initiated, the pipe is near room temperature. The weld bead profile at the start (Figure 60 and Figure 61) slowly changes as a steady-state temperatures are built in the material based on the heat input of each welding procedure. In general, most weld starts appeared more convex based on the low starting material temperature. Note that test R-04 was overlapped on test R-03 to provide a larger deposit layer in Figure 61.

Figure 60 - Test R-01 at 12:00 Showing Poor Stop-Start Tie-In

Figure 61 - Tests R-03 and R-04 at 12:00 Showing Better Stop-Start Overlap.

The preferred welding parameters were based on optimizing the bead shape in the steady state (Figure 62). For internal repair of pipelines, a programmable weld controller could be used to use higher welding heat input at the weld start. This would provide better weld bead start quality. Once welding the start parameters could be ramped in the steady-state parameters to provide uniform bead shape.

Figure 62 - Tests R-01 and R-02 at 3:00 Showing Steady-State Bead Shape

Table 8 contains the welding parameters for the weave bead procedures used. Wire feed speeds varied from 5.08 mpm (200 ipm) to 6.35 mpm (250 ipm). This was better than preliminary tests with the Bortech system, which were at 4.45 mpm (175 ipm) and resulted in stringer beads that had a ropy appearance.

Weld No.	Specimen No.	Wire Feed Speed mpm (ipm)	Voltage (Trim)	Travel Speed mmpm (ipm)	Weave Amplitude mm/side (in/side)	Weave Frequency (Hz)	Dwell Time (seconds)	Comment
1	R-01	5.08 (200)	0	76.2 (3)	9.9 (0.39)	0.6	0.6	Good for a narrow repair.
2		5.08 (200)	0	127 (5)	25.4 (1.00)	0.6	0.2	Too fast. Zigzag pattern results.
3	R-02	6.43 (253)	-4	25.4 (1)	25.4 (1.00)	0.1	0.6	• Bad at overhead position • Turned voltage to -4 • Dwell is not needed
4	R-03	6.43 (253)	-4	25.4 (1)	25.4 (1.00)	0.1	0.0	6 mm (0.25 in.) overlap at overhead position to tie two welds together - porosity resulted.
5	R-04	6.43 (253)	-4	25.4 (1)	25.4 (1.00)	0.1	0.0	• 6 mm (0.25 in.) overlap at overhead and flat positions. • Centerline is 22 mm (0.88 in.) from previous weld edge (3 mm (0.125 in.) circumferential overlap). • Good circumferential tie on uphill side. • Poor circumferential tie on downhill side. • Need more wire feed speed due to bad fusion on downhill side
6	R-05	7.62 (300)	-4	25.4 (1)	25.4 (1.00)	0.1	0.0	• 6 mm (0.25 in.) overlap at every 30 degrees. • See Table 9 for tie-in quality at each position

Table 8 - Welding Parameters for Specimens R-01 through R-05

Table 9 contains the tie-in quality at each clock position for specimen R-05.

Position (clock)	Tie In Quality (poor/OK/good)
12:00	Poor
1:00	Poor
2:00	Poor
3:00	Poor
4:00	OK
5:00	Good
6:00	Good
7:00	Robot problem
8:00	Good
9:00	Good
10:00	Good
11:00	OK

Table 9 - Tie-In Quality at Each Clock Position for R-05

To further improve starting bead shape some additional tests were performed using 7.62 mpm (300 ipm) wire feed speed (Figure 63). These tests were used by the technician to study the precise location for starting on a stop and to evaluate gravity effects. As shown by these tests, the use of higher wire feed speeds which produce higher heat input can be used to improve start bead shape. No additional procedures were developed with the 6-axis robot.

12:00 – Too Much Overlap

1:00 – Too Much Overlap

2:00 – Slightly Better

3:00 – Some Convexity

4:00 – Okay

5:00 – Good

6:00 – Good

7:00 – Bad Appearance Due
Robot Program Error

8:00 – Good

9:00 – Good

10:00 – Good

11:00 – Okay

Figure 63 - Tie-In Tests Using Parameters R-05 Every 30º Around One Ring Deposit

Comprehensive Test Program

A comprehensive test program was developed to evaluate the two most feasible potential repair methods of carbon fiber-reinforced composite liner repair and weld deposition repair based on the pipeline operator survey, input from NETL, physical testing to date, corrosion being the most common pipeline failure, and rupture due to excessive internal pressure being the failure mechanism of corrosion.

From the operator survey, it was determined that pipe outside diameter sizes range from 50.8 mm (2 in.) through 1,219.2 mm (48 in.). The most common size range for 80% to 90% of operators surveyed is 508 mm to 762 mm (20 in. to 30 in.), with 95% using 558.8 mm (22 in.) pipe. Both 558.80 mm (22 in.) diameter by 7.92 mm (0.312 in.) wall, API 5L-Grade B pipe and 508 mm (20 in.) diameter by 6.35 mm (0.250 in.) wall, API 5L-X52 pipe sections were obtained from Panhandle Eastern.

The test program considered a range of damage types, both internal and external, that are typical of those encountered in pipelines. The U. S. Department of Transportation, Research and Special Programs Administration, Office of Pipeline Safety, compiles statistics on pipeline failure causes[5] which are posted on their web site located at *http://primis.rspa.dot.gov/pipelineInfo/stat_causes.htm*. During 2002-2003, DOT statistics indicate that for natural gas transmission pipelines the largest contributor to pipeline damage was clearly corrosion (as shown in Table 10). Eventually, the wall thickness decreases to the point where it is not sufficiently large enough to contain the stresses from the internal pressure and the pipeline will rupture or burst.

Reported Cause	Number of Incidents	% of Total Incidents	Property Damages	% of Total Damages	Fatalities	Injuries
Excavation Damage	32	17.9	$4,583,379	7.0	2	3
Natural Force Damage	12	6.7	$8,278,011	12.6	0	0
Other Outside Force Damage	16	8.9	$4,687,717	7.2	0	3
Corrosion	46	25.7	$24,273,051	37.1	0	0
Equipment	11	6.1	$3,958,904	6.0	0	5
Materials	36	20.1	$12,130,558	18.5	0	0
Operation	5	2.8	$286,455	0.4	0	2
Other	21	11.7	$7,273,647	11.1	0	0
Total	179		$65,471,722		2	13

Table 10 - 2002-2003 Natural Gas Transmission Pipeline Incident Summary by Cause

Given the fact that corrosion was the most significant contributor to natural gas pipelines failures during 2002 and 2003, the two most common types of corrosion, general corrosion and a deep/isolated corrosion pit (both with a 30% reduction in burst pressure) were selected for

repair process evaluation. Both types of corrosion damage were introduced into pipe sections with a milling machine. Using a ball end mill, long shallow damage representative of general corrosion (as shown in Figure 12) was originally introduced into pipe specimens. Using an end mill with rounded corners, short, deep damage representative of a deep isolated corrosion pit (as shown in Figure 13) was introduced pipe specimens as well. Over time, external corrosion will continue to decrease pipeline wall thickness.

The selected configuration for simulated corrosion damage for 558.80 mm (22 in.) pipe is shown in Figure 64. The dimensions for the 20 in pipe were appropriately scaled down. The selected design for simulated corrosion damage for 508 mm (20 in.) pipe is shown in Figure 65.

Figure 64 - Selected Configuration of Simulated Damage for 558.80 mm (22 in.) Diameter Pipe Sections
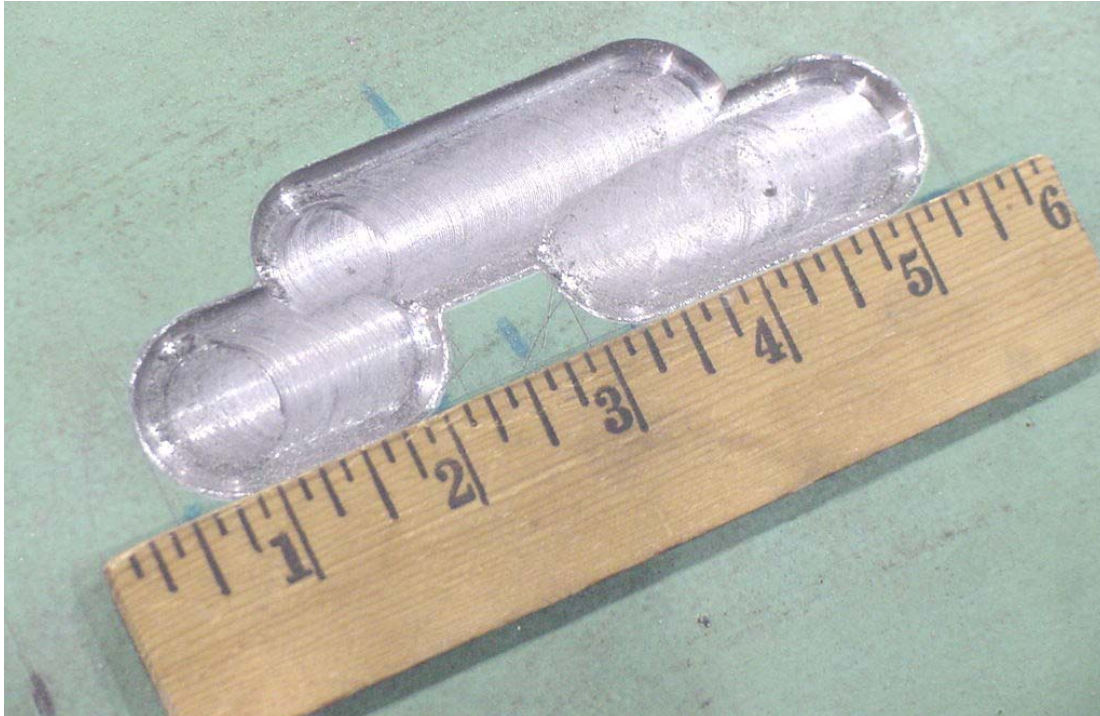
Figure 65 - Selected Configuration of Simulated Damage for 508 mm (20 in.) Diameter Pipe Sections

The dimensional data and RSTRENG-predicted burst pressures for the selected simulated corrosion damage configuration for internal repair evaluation trials is shown in Table 11.

Pipe Outside Diameter	558.80 mm (22 in.)	508 mm (20 in.)
Wall Thickness	7.92 mm (0.312 in.)	6.35 mm (0.250 in.)
Pipe Material	API 5L-Grade B	API 5L-X52
Type of Damage	Simulated Corrosion Defect	Simulated Corrosion Defect
Damage Length	190.50 mm (7.5 in.)	127.00 mm (5 in.)
Damage Depth	3.96 mm (0.156 in.)	3.45 mm (0.136 in.)
Pressure corresponding to 100% SMYS	6.84 MPa (992 psi)	8.96 MPa (1,300 psi)
Damage as % of Wall Thickness	50%	54%
RSTRENG-predicted burst pressure for pipe with simulated damage	5.15 MPa (747 psi)	6.72 MPa (974 psi)
RSTRENG-predicted burst pressure compared to pressure at 100% SMYS	75%	75%

Table 11 - Dimensional Data and RSTRENG Predicted Burst Pressures for Simulated Corrosion Damage Selected for Internal Repair Evaluation Trials

Based on the preliminary fiber-reinforced liner and weld metal deposition repair trials conducted in the first six months of this project, the test program was consequently designed to evaluate full-scale pipe sections with simulated corrosion damage repaired with both carbon fiber-reinforced composite liner repairs and weld deposition repairs that will be subsequently hydrostatic pressure tested until rupture. Additionally, full-scale pipe sections in the virgin (i.e., un-damaged) condition and with un-repaired simulated corrosion damage were also hydrostatically tested until rupture to establish baseline performance data against which to compare the performance of both repair technologies.

According to the Project Management Plan[2], Subtask 4.2 activities contain the development of a detailed test matrix to enable the selected repair methods to be evaluated over a range of typical operating conditions. Since physical testing to date has shown that carbon fiber-reinforced liner repair is clearly superior to weld deposition repair, it is more appropriate for this activity to be incorporated into the activities for Subtask 4.4 (Internal Repair Evaluation Trials) and to be developed solely for the application of carbon fiber-reinforced liner repair.

4.2 - Simulation and Analysis of Potential Repair Methods

In previous work for PRCI[6], finite element analysis (FEA) was performed to simulate external weld deposition repair of internal wall loss. Additional engineering analysis was planned to simulate internal weld deposition repair of external wall loss.

Prior to the initial trials for fiber-reinforced composite repairs, RolaTube conducted FEA to determine the required properties of the liner material. Again, postmortem analysis of the pipe section damage indicates that the difference in modulus of elasticity between the steel and the original glass fiber-reinforced liner material prevents the liner from carrying its share of the load.

Realistic combinations of composite material and thickness were determined for use in liner systems for internal repair of natural gas transmission pipelines.

Pipeline repairs that use internal addition of material are advantageous for many circumstances where access to the external surface of the pipe is restricted. Transportation of any material that will be added to the pipe wall must be considered, since it must ultimately be introduced from outside the pipe wall. Composites offer the opportunity to tailor the properties of the liner material in different directions to allow the material to be fit through the inside of the pipe and then be reshaped so it can be placed against the wall in the area where repair is desired.

Since repair is contemplated most often for external corrosion that exceeds the allowable limit sizes, we should consider that corrosion on the external surface may continue after the emplacement of the liner. As the external corrosion continues, the situation will get closer and

closer to that where only the liner carries the stresses from the internal pressure in the pipe. A simple case can be used for estimation where the entire steel pipe has been lost to external corrosion and only the liner is left to carry the external stress.

We can choose an initial case in the middle of the commonly used range for transmission pipelines: a 508 mm (20 in.) outside diameter pipe with a 6.35 mm (0.25 in.) wall thickness made from X-65. For this pipeline, the additional liner material should not be so thick as to prevent subsequent examinations of the adjacent steel pipeline by internal inspection devices. This roughly limits the thickness of the liner t_c to less than 12.7 mm (0.5 in.) thickness.

We can define several criteria for the acceptability of the liner repair. One will involve the strength of the liner under a maximum pressure. One simple test case is that the liner should not be at greater risk of bursting than the remote un-repaired pipe under the pressure to reach a stress equal to the standard minimum yield strength of the pipe material. Using Barlow's formula, the pressure P to reach this hoop stress in the remote pipe is SMYS t/R or 11.3 MPa (1,646 psi).

Composite materials differ from steel in the expected stress-strain relationship. The composite liner material would be designed to be strong both in the axial and hoop directions. In a strong direction, the composite will have a much lower peak strain before failure than steel, but the stress-strain curve up to that failure point will be much closer to elastic.

Figure 66 shows some estimates of the ranges of tensile strength and modulus for carbon fibers. The strength goes down as the modulus increases, a relationship that can be approximated by a linear relationship between the fiber modulus E_f and the tensile strength of the fiber σ_{fu}

$$\sigma_{fu} = 4{,}140 MPa - 1{,}380 MPa \times \left(\frac{E_f}{29{,}300 MPa} \right)$$

Equation 1 - Tensile Strength of the Fiber σ_{fu} in MPa

$$\sigma_{fu} = 600 ksi - \left(\frac{200 \times E_f}{42{,}500} \right)$$

Equation 2 - Tensile Strength of the Fiber σ_{fu} in ksi
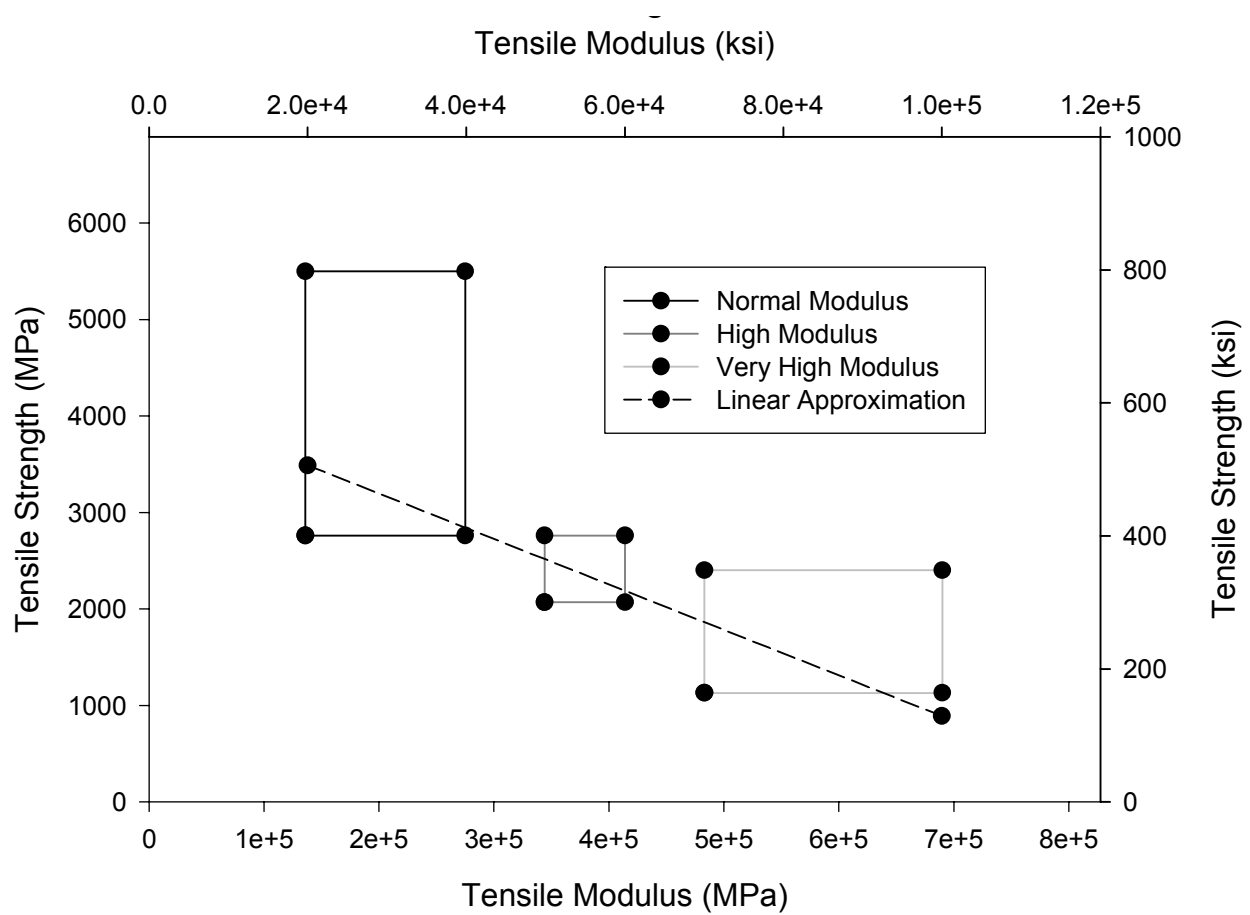
Figure 66 - Relationship Between Modulus and Strength for Carbon Fibers

The tensile strength and modulus of the composite can be estimated in the strong direction as 60% of the fiber strength and modulus, respectively. It will be appropriate to use a safety factor (SF) on failure strength in design to keep the strain well below the failure level.

Now the design condition for the composite becomes

$$P < \frac{SF \times 0.6 \times \sigma_{fu} \times t_c}{R - \dfrac{t}{2} - \dfrac{t_c}{2}}$$

Equation 3 - Pressure to Reach Stress Equal to the SMYS of the Pipe Material

Once SF has been set (with a value of 0.9) then we can determine the relationship between σ_{fu} and t_c that defines the minimum allowable based on the values chosen above:

$$\sigma_{fu} > 10,500 MPa\text{-}mm \times \left(\frac{1}{t_c}\right) - 10.5 MPa$$

Equation 4 - Minimum Allowable Tensile Strength of the Fiber σ_{fu} in MPa

$$\sigma_{fu} > 60.2 ksi - in \times \left(\frac{1}{t_c}\right) - 1.524 ksi$$

Equation 5 - Minimum Allowable Tensile Strength of the Fiber σ_{fu} in ksi

The fiber modulus can thus be given a maximum value using the linear approximation given above. This function is plotted in Figure 67.

$$E_f < \left(\frac{293,000}{1,380}\right) \times \left[4,140 - \left\{10,500 \times \left(\frac{1}{t_c}\right) - 10.5\right\}\right] \quad \text{for } t_c \text{ in mm}$$

Equation 6 - Maximum Fiber Modulus in MPa

$$E_f < \left(\frac{42,500}{200}\right) \times \left[600 - \left\{60.2 \times \left(\frac{1}{t_c}\right) - 1.524\right\}\right] \quad \text{for } t_c \text{ in inches}$$

Equation 7 - Maximum Fiber Modulus in ksi

If the fiber modulus is above the line in Figure 67, then the strength of the fibers will be too low to achieve the required strength in the composite.
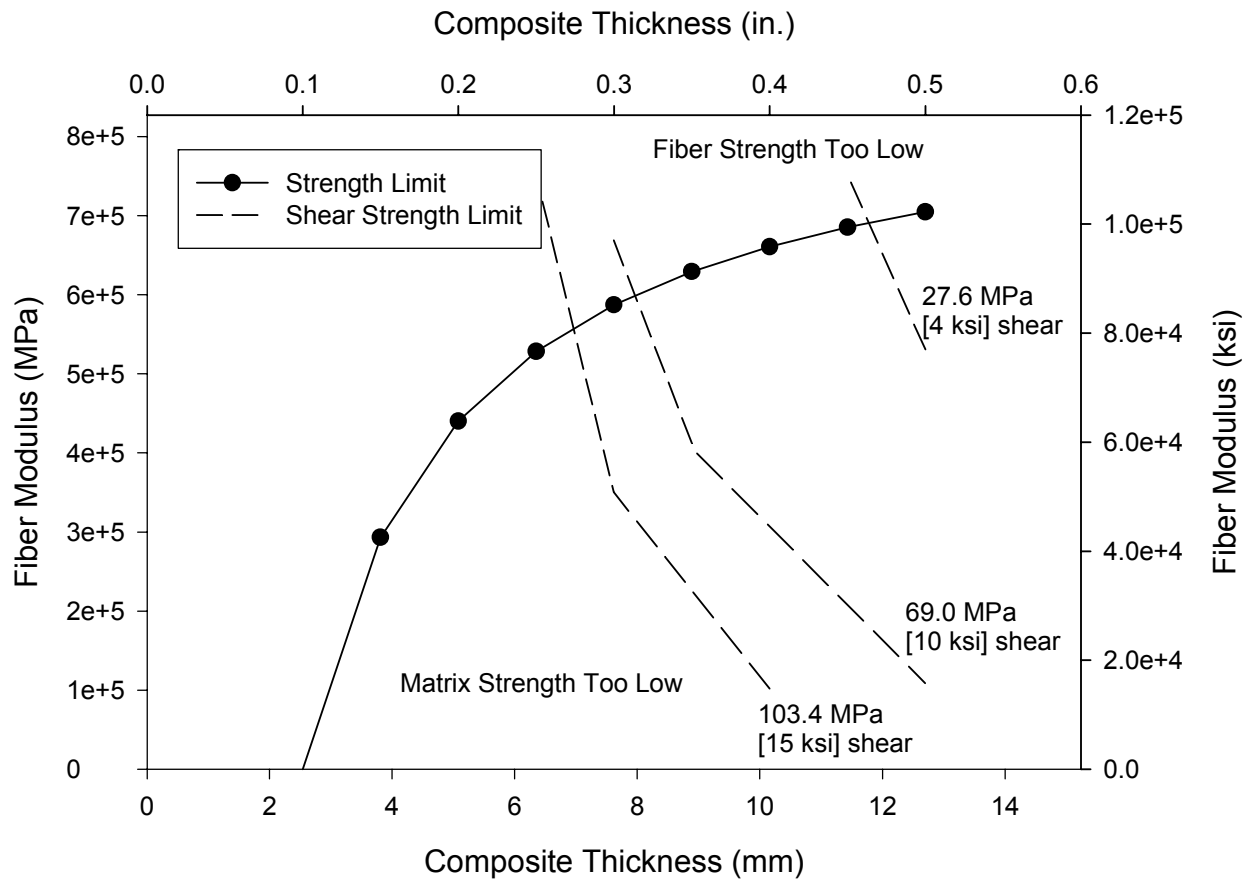
Figure 67 - Design Space for Composite Liner

This both limits the minimum thickness of the composite and limits the use of the highest modulus fibers, since they have lower ultimate strengths.

There can also be a problem with failure in shear of the matrix material between the layers of fibers. The simple case described above does not have shear between the fibers, but any case where the steel thickness varies in the hoop direction will have to transfer loads back and forth into the composite and induce shear where those transfers occur.

Again, we assume a simple case. Here the case is a relatively abrupt transition from the full wall thickness of steel to no steel remaining over a small sector of the circumference, with long axial length. In this case, we have to transfer all of the load that was carried by the steel into the composite on one side of the loss of wall thickness and back into the steel on the other side. We can assume that all of the transfer occurs within a distance of four times the composite thickness, centered on the transition of the steel wall thickness to zero. Then we can estimate the shear between the composite layers based on an even transfer of the moment across this distance.

The moment per unit length is PRc, where c is a function of the thickness of pipe t_s and composite t_c and the moduli of the materials E_s and E_c. The c function can be written as

$$c = \frac{t_s \times E_s \times \left(\frac{t_s}{2} + \frac{t_c}{2}\right)}{(t_s \times E_s) + (t_c \times E_c)}$$

Equation 8 - c as a Function of the Thickness of Both the Pipe and Liner, and the Moduli of Both the Pipe and Liner

The shear stress τ is as function of the shear force per unit length V

$$\tau = \frac{\left(\frac{4}{3}\right) \times V}{t_c}$$

Equation 9 - Shear Stress as a Function of Shear Force

where

$$V = \frac{P \times R \times c}{2 \times t_c}$$

Equation 10 - Shear Force per Unit Length

The shear stress must not exceed the shear resistance of the matrix material in the composite. Some examples of shear resistance have been chosen and included in Figure 67.

The combination of the two design cases indicates that there is an optimum modulus of the fibers that allows the smallest thickness to be used. This optimum modulus is a function of the shear strength of the matrix material as well.

The second design case could be refined by finite element modeling, which would better estimate the peak shear forces in the composite.

Two economic limits should also be considered with carbon fiber composites. Higher modulus of the composite can be achieved by choosing high modulus fibers, but at increasing cost. Nevertheless, the more expensive manufacturing process for the highest modulus fibers has prevented wide scale use in infrastructure. The alternative described above is to go to larger

thickness. Nevertheless, the larger thickness must be created in the composite by the addition of more sheets or "plies" of the fibers. As the number of plies increases, the manufacturing difficulties multiply. The "comfort level" for number of plies would today probably be less than that which would be needed for a 12.7 mm (0.5 in.) thick composite liner.

The assessment above has only related to the hoop stress resistance of the composite. Axial strain resistance is also available from the composite because both the axial and hoop directions are strengthened by the fibers.

Composite liners need both high fiber modulus and high shear strength of the matrix, above that for many thermoplastics, to resist the types of shear stresses that can happen in composite liners. There are limits to how high the modulus of the fibers should go, because the strength drops off for the highest modulus fibers.

4.3 - Internal Repair Evaluation Trials

Evaluations of potential repair methods focused on fiber-reinforced composite liner repairs and weld deposition repairs. Areas of simulated damage were introduced into a 508 mm (20 in.) diameter pipe section, which was subsequently repaired with carbon fiber-reinforced liners. The repaired pipe section was then hydrostatically tested until failure. An additional 558.8 mm (22 in.) diameter pipe section with simulated damage was subsequently repaired using the GMAW process applied from the inside of the pipe. This pipe section was also hydrostatically tested until failure.

Fiber-Reinforced Liner Repairs

From a pipe provided by Panhandle Eastern, a section of 508 mm (20 in.) diameter pipe with simulated corrosion damage was used to evaluate a carbon fiber-reinforced liner. EWI procured raw carbon fiber material and fabricated a 11.4 mm (0.45 in.) thick reinforcement patch using a "wet lay-up" process with a vinylester resin system. As compared to the glass fiber-reinforced composite, carbon fiber-based composite materials have a much higher modulus of elasticity. The modulus of elasticity for commercial grade raw carbon fiber material is in the 206.8 GPa (30×10^6 psi) range, but this is reduced significantly when a matrix material is introduced. High grade raw carbon fiber materials have a modulus of elasticity that is in the 344.7 to 413.7 GPa (50 to 60×10^6 psi) range; however, these high grade raw carbon fiber materials are expensive and scarce. None the less, it may be possible to design a liner material that, when the matrix material is introduced, has a modulus of elasticity on the order of 95% of that for steel.

The cost of a liner composed of high-grade raw carbon fiber material will initially be high. The results of the survey of pipeline operators suggests that such a repair may still be useful in spite of the high cost for river crossings, under other bodies of water (e.g., lakes and swamps), in

difficult soil conditions, under highways, under congested intersections, and under railway crossings.

When the glass/polypropylene liner material was evaluated, it was found to be generally ineffective at restoring the pressure containing capabilities of the pipe. The important contributing physical property for a composite repair device is assumed to be an intrinsic modulus approximating that for steel. Based on materials cost and availability, a true match was not possible, so the alternative was to develop a composite having an attainable estimated modulus and adjust section thickness to achieve the desired stiffness.

The second issue is the ability to "access" that stiffness in the form of the composite physical properties. The limiting factor in composite failure is often interlaminar shear strength. A reaction to radial flexure will be a reacted shear stress that will attempt to separate the fabric lamina at the weak link, the resinous interface between fabric layers. A typical value for a "good" composite is an interlaminar shear strength of about 51.7 MPa (7,500 psi).

Taking these two requirements together, engineering analysis was employed to arrive at the composite requirements based on the assumed values for economical carbon fiber reinforcement with a vinylester resin system (see Results and Discussion section for Subtask 4.3 - Simulation and Analysis of Potential Repairs Methods). It was determined that the patch should be on the order of 11.4 mm (0.45 in.) thick to approximate the stiffness of the steel while still maintaining an interlaminar shear strain below the 51.7 MPa (7,500 psi) benchmark.

After two weeks of cure time, the pipe section with the EWI fabricated patch was hydrostatically tested until failure (Figure 68). The resultant burst pressure was 15.13 MPa (2,194 psi) which is 122% of pressure corresponding to 100% of specified minimum ultimate tensile strength. Figure 69 is a closer view of the failure initiation site. Figure 70 clearly shows that the failure was caused by interlaminar shear mostly between the anti-corrosion glass layer and the carbon layer (1→2 layer interfacial failure is common in composites). There was no evidence of disbonding between the pipe and the composite liner.

Figure 68 - Pipe With Carbon Fiber-Reinforced Liner Repair After Burst Test

Figure 69 - Failure Initiation Site For Burst Tested Pipe With Carbon Fiber-Reinforced Liner Repair

Figure 70 - Magnification of Carbon Fiber-Reinforced Patch After Burst Test

Table 12 contains the RSTRENG predicted and measured burst pressures for pipe repaired with a carbon fiber-reinforced liner.

Composite Repair	Burst Pressure		Failure Location
	(MPa)	(psi)	
RSTRENG Prediction	6.72	974	n/a
Burst Test	15.13	2,194	Center of reduced area

Table 12 - Predicted and Measured Burst Pressures for Pipe with A Carbon Fiber-Reinforced Liner Repair

The burst pressure for the pipe repaired with a carbon fiber reinforced liner is much higher than the RSTRENG predicted burst pressure for an un-repaired pipe. This result must be viewed while taking into account the results of the additional testing that was performed on virgin (i.e., un-damaged) pipe and on pipe with un-repaired simulated corrosion damage, however. The results of this testing and an overall comparison of all burst test results are located in the Results and Discussion section for Subtask 4.4 - Internal Repair Evaluation Trials under the heading for Baseline Pipe Material Performance.

This testing was an excellent evaluation of a carbon fiber-reinforced liner material. The patch design requires optimization, perhaps allowing a tapered design or smaller dimensions. The vacuum-bagging process also requires refinement. A Vacuum Assisted Resin Transfer Molding (VARTM) approach would be optimal as it would produce far better fiber compaction and would allow the production of more complex patch designs

The results of these trials indicate that the use of carbon fiber-reinforced liners is promising for internal repair of gas transmission pipelines. Fiber reinforced composite repairs applied to the outside of exposed pipelines have become commonplace in the gas transmission pipeline industry. Based on the results of these trials, the application of this technology to internal repair appears to be feasible, although further development is required to achieve the required material properties. It is anticipated that higher grade raw carbon fiber materials will become more widely available in the future. Further development is also required to optimize the design of the carbon fiber liner/patch. Another promising aspect of internal pipeline repair using fiber reinforced composite materials is that there is no apparent technical limitation for performing the repairs while the pipeline remains in service.

Weld Deposition Repairs

EWI conducted two weld metal deposition studies. The first evaluation was to determine the feasibility of making weld deposition repairs on the inside diameter (ID) of a pipeline to replace metal loss on the outside diameter (OD) due to corrosion damage. The second evaluation was to determine the effect of methane in the welding environment on weld quality as the amount of methane was varied in the shielding gas.

To evaluate internal weld metal deposition repairs to replace metal loss on the OD due to corrosion damage, two layers of weld metal were deposited inside a section of 558.8 mm (22 in.) diameter API 5L-Grade B pipe that was incased in a dirt box filled with soil.

After two layers of weld metal were deposited inside the pipe section, several ultrasonic thickness measurements were subsequently taken to confirm that the weld deposition layers restored the pipe wall back to the original thickness. See Figure 71 for the thickness measurement locations.
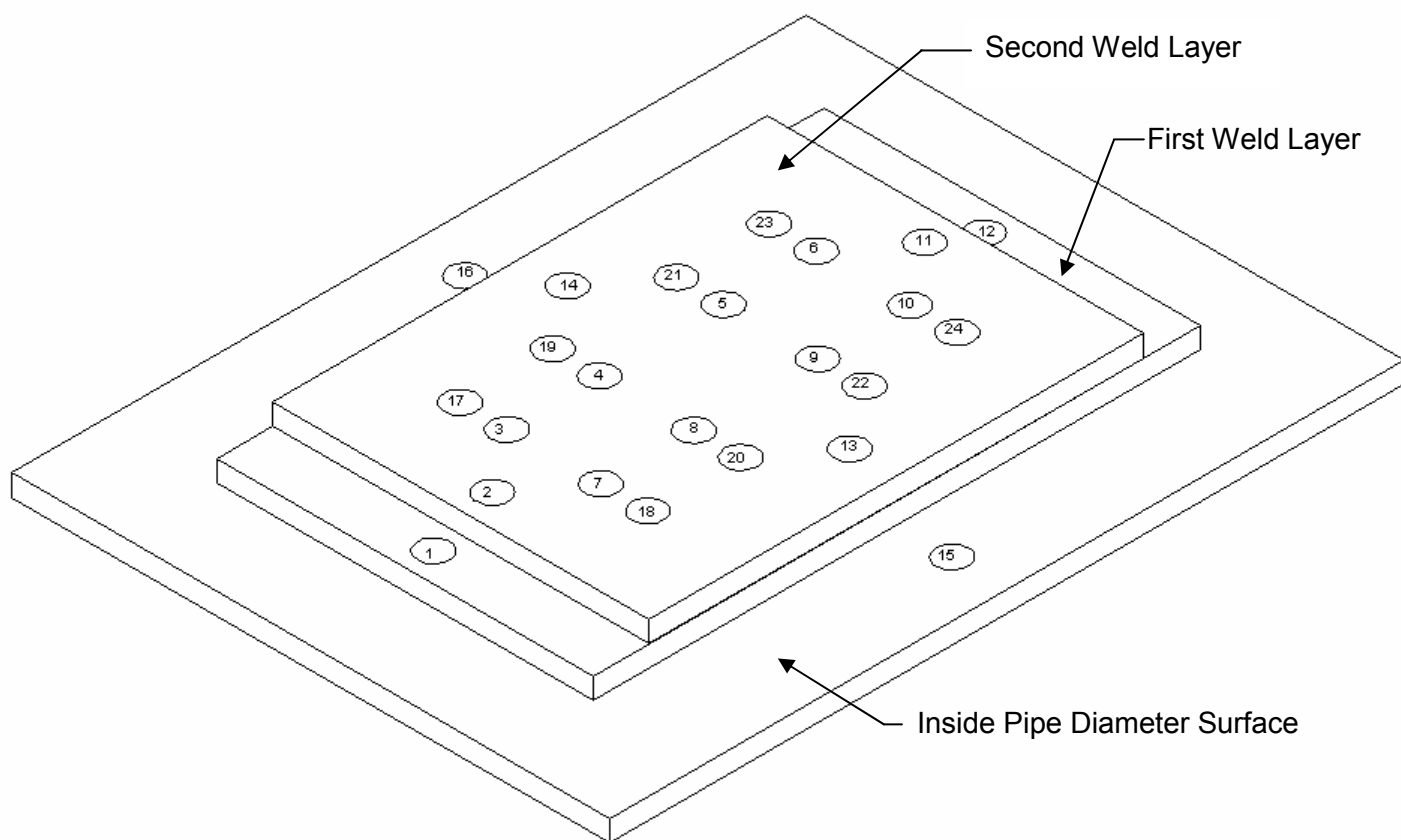
Figure 71 - Ultrasonic Thickness Measurement Locations on Weld Deposition Repair

Spacing of the ultrasonic measurements on the second weld layer were close enough to assure that the entire simulated corrosion area was measured. Locations 15 and 16 were designated as reference measurements.

There are five locations that had thickness values less than that of reference points 15 and 16 (as seen in Table 13). As a consequence, these areas were ultrasonically scanned to determine the cause of the irregularities. It was determined that the irregularities were caused by lack-of-fusion defects between the weld toes of the first layer and the inside diameter of the pipe. These defects were oriented along the circumferential direction of the pipe.

Defects oriented in the longitudinal direction have a tendency to fail from hoop stress (i.e., pressure loading) and must be reinforced in the circumferential direction. Defects oriented in the circumferential direction have a tendency to fail from axial stresses (due to pipeline settlement, etc.) and must be reinforced in the longitudinal direction. The irregularities found in the weld deposition layers were considered inconsequential to hydrostatic testing given their size and circumferential orientation, therefore, hydrostatic burst testing was conducted on the pipe section without repairing the irregularities. Additional ultrasonic measurements were taken

at four locations with the transducer to the side of the defect. These measurements are shown to the right of the irregular defective measurements (to the right of the slash) in Table 13. The four additional measurements were in excess of reference measurements 15 and 16.

Thickness Measurement Location in Figure 71	Thickness Measurement		Comments
	mm	inches	
1	10.67	0.420	
2	13.13	0.517	
3	5.36 / 9.14	0.211 / 0.360	Lack-of-Fusion
4	13.21	0.520	
5	5.28 / 13.06	0.208 / 0.514	Lack-of-Fusion
6	9.27	0.365	
7	9.37	0.369	
8	9.22	0.363	
9	5.84 / 9.35	0.230 / 0.368	Lack-of-Fusion
10	9.12	0.359	
11	13.67	0.538	
12	10.59	0.417	
13	13.41	0.528	
14	5.20 / 13.34	0.205 / 0.525	Lack-of-Fusion
15	7.89	0.311	Reference Measurement
16	8.18	0.322	Reference Measurement
17	13.21	0.520	
18	9.37	0.369	
19	13.46	0.530	
20	9.25	0.364	
21	5.46	0.215	Lack-of-Fusion
22	9.39	0.370	
23	13.97	0.550	
24	9.37	0.369	

Table 13 - Ultrasonic Thickness Measurements at Locations in Figure 71

The area of simulated corrosion on the outside pipe surface is shown in Figure 72 after internal weld deposition repair.

Figure 72 - Simulated Corrosion on Outside of Pipe After Internal Weld Deposition Repair

After the box with soil was removed from the weld repaired pipe section, an impression of the corrosion damage was left in the soil as shown in Figure 73. The outline of the weld deposition is also clearly visible where the asphalt coating melted and transferred to the surrounding soil during the welding process.

Figure 73 - Dirt That Was In Contact With Pipe During Internal Weld Deposition Repair

Upon further examination, the outside pipe surface (opposite the internal weld repair) exhibited a dent (a.k.a. welding distortion) as a result of the weld heating and cooling cycles. In Figure 74, a red string is used as a reference against which to measure the extent of the distortion. The red string indicates where the outside surface of the pipe was before welding. The yellow box indicates the location of the simulated corrosion. Figure 75 contains magnified pictures from the middle and ends of the dented area of pipe.
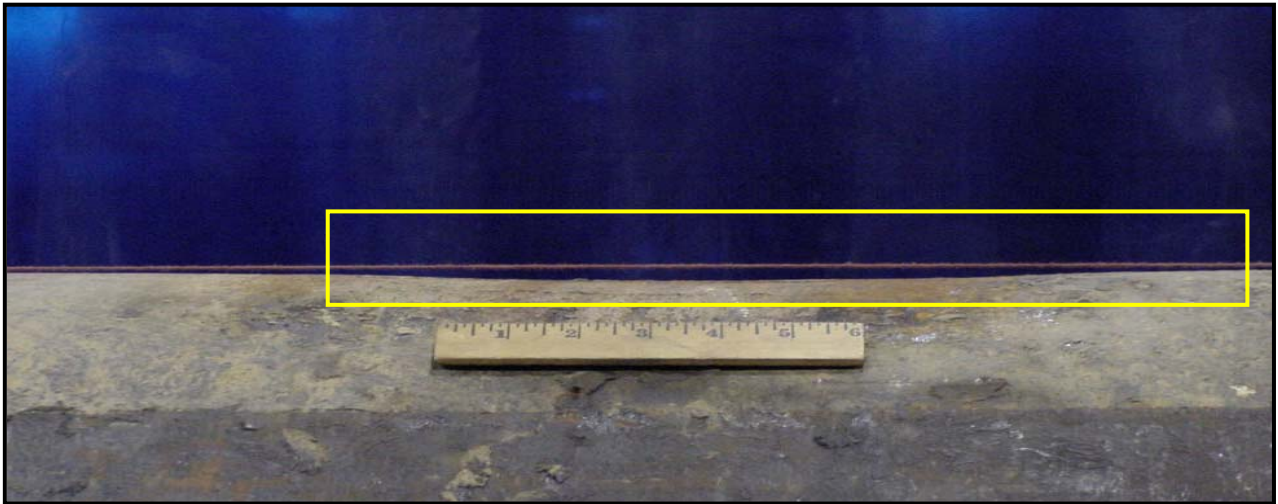
Figure 74 - Profile of Dent in Outside Pipe Surface After Internal Weld Deposition Repair
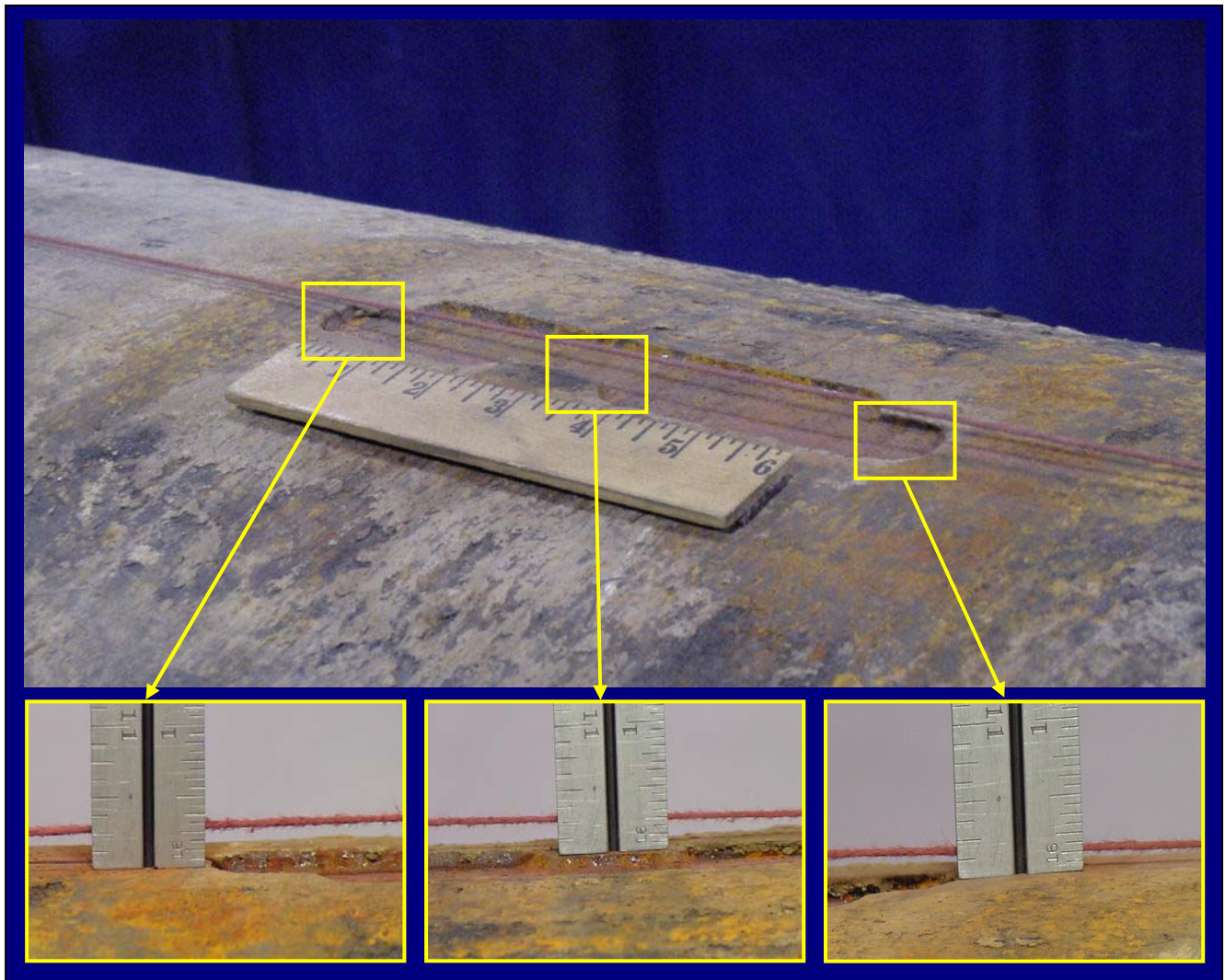
Figure 75 - Magnified Pictures of Dent at Ends and Middle of Simulated Damage

Figure 76 - Pipe Section with Internal Weld Deposition Repair After Hydrostatic Burst Test

Table 14 contains the predicted and actual burst pressure values.

Pipe Outside Diameter	558.80 mm (22 in.)
Wall Thickness	7.92 mm (0.312 in.)
Pipe Material	API 5L-Grade B
Type of Damage	Simulated Corrosion Defect
Damage Length	190.50 mm (7.5 in.)
Damage Depth	3.96 mm (0.156 in.)
Pressure corresponding to 100% SMYS	6.84 MPa (992 psi)
Damage as % of Wall Thickness	50%
RSTRENG-predicted burst pressure for pipe with damage	5.15 MPa (747 psi)
RSTRENG-predicted burst pressure compared to pressure at 100% SMYS	75%
Measured burst pressure for pipe with damage following repair	9.68 MPa (1,404 psi)

Table 14 - Hydrostatic Bust Test Results for Internal Weld Deposition Repair Specimen

The burst pressure for the pipe repaired with using weld deposition is much higher than the RSTRENG predicted burst pressure. As before, this result must be viewed while taking into account the results of the additional testing that was performed on virgin (i.e., un-damaged) pipe and on pipe with un-repaired simulated corrosion damage. The results of this testing and an overall comparison of all burst test results are located in the Results and Discussion section for Subtask 4.4 - Internal Repair Evaluation Trials under the heading for Baseline Pipe Material Performance.

During any arc welding operation, the material being welded is exposed to temperatures that range from ambient to well above the melting temperature 1,536°C (2,736°F). When steel at high temperature is exposed to a hydrocarbon gas (such as methane), carburization can occur. When steel at temperatures above 1,130°C (2,066°F) is exposed to methane, eutectic iron can form as the result of diffusion of carbon from the methane into the steel. In previous work at EWI,[7] in which welds were made on the outside of thin-wall pipe containing pressurized

methane gas (Figure 77, Figure 78, and Figure 79), carburization and the formation of thin layer of eutectic iron occurred (Figure 80 and Figure 81).
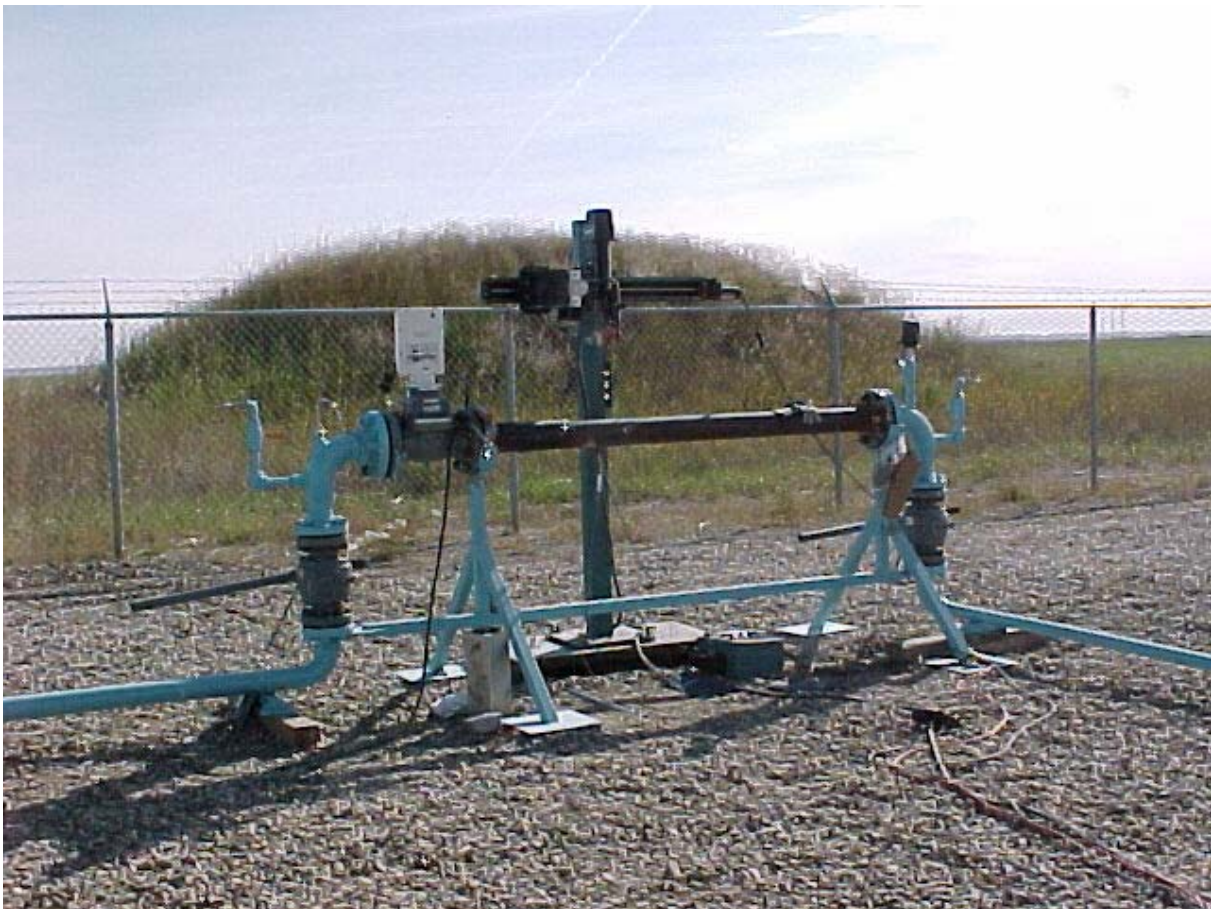
Figure 77 - Experimental Set-Up for Welding onto Thin-Wall Pipe containing Pressurized Methane Gas

Figure 78 - External Appearance of Welds Made on 3.2 mm (0.125 in.) Thick Pipe with Methane Gas at 4.5 mPa (650 psi) and 6.1 m/sec (19.9 ft/sec) Flow Rate
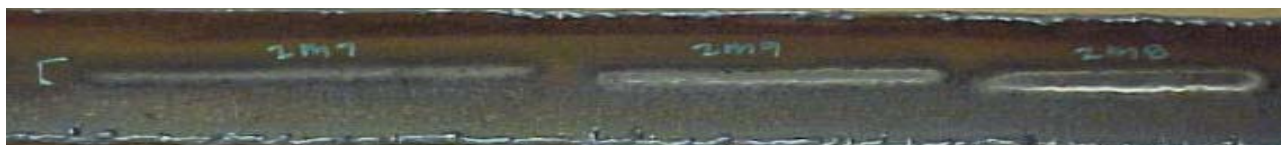
Figure 79 - Internal Appearance of Welds Shown in Figure 78
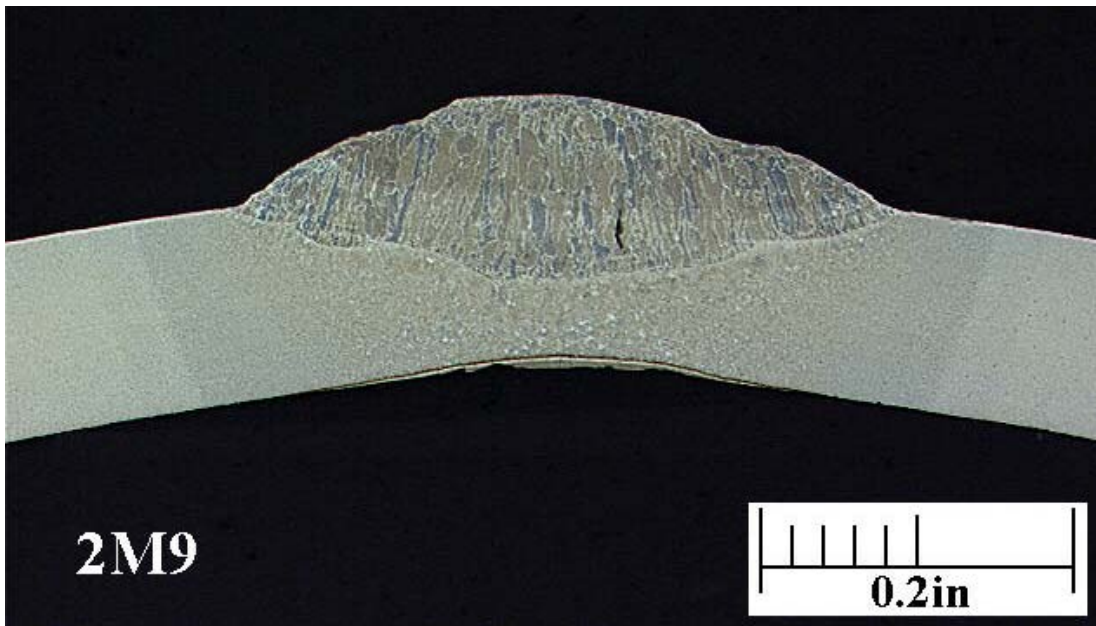
Figure 80 - Metallographic Section through Weld 2M9 (middle weld shown in Figure 78 and Figure 79)
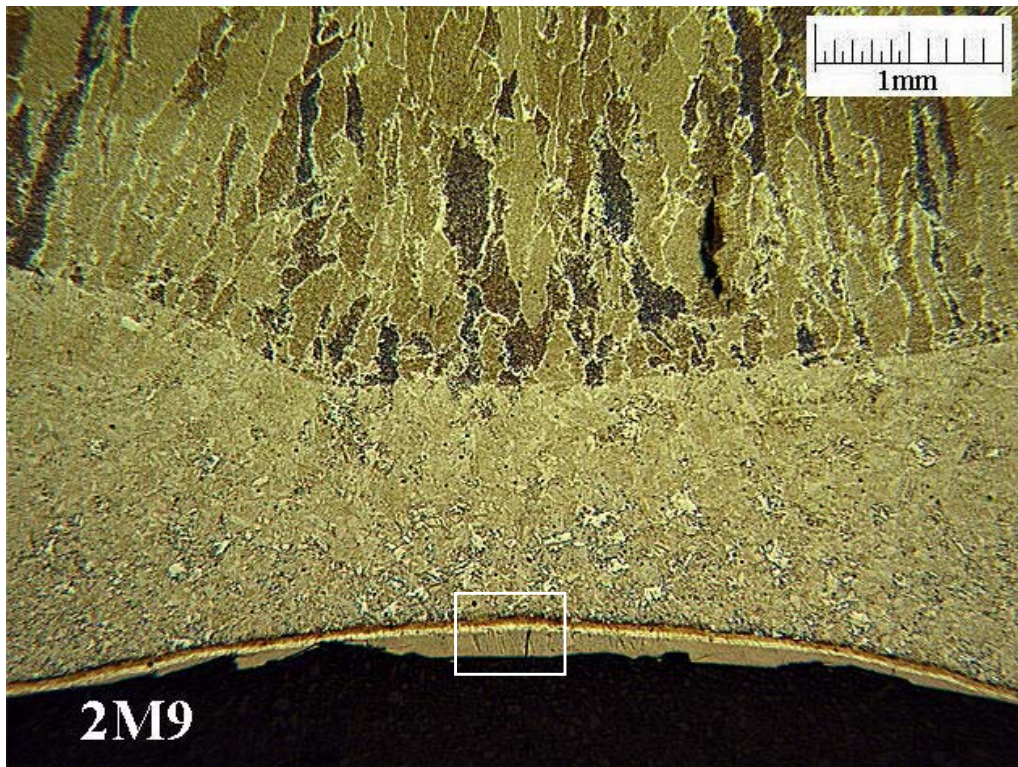
Figure 81 - Eutectic Iron Layer at Inside Surface of Metallographic Section through Weld 2M9

This phenomenon was previously reported by Battelle during experiments with liquid propane.[8] There were also small cracks associated with the eutectic iron layer (Figure 82), which were attributed to the limited ductility of eutectic iron. This subtask is complete.
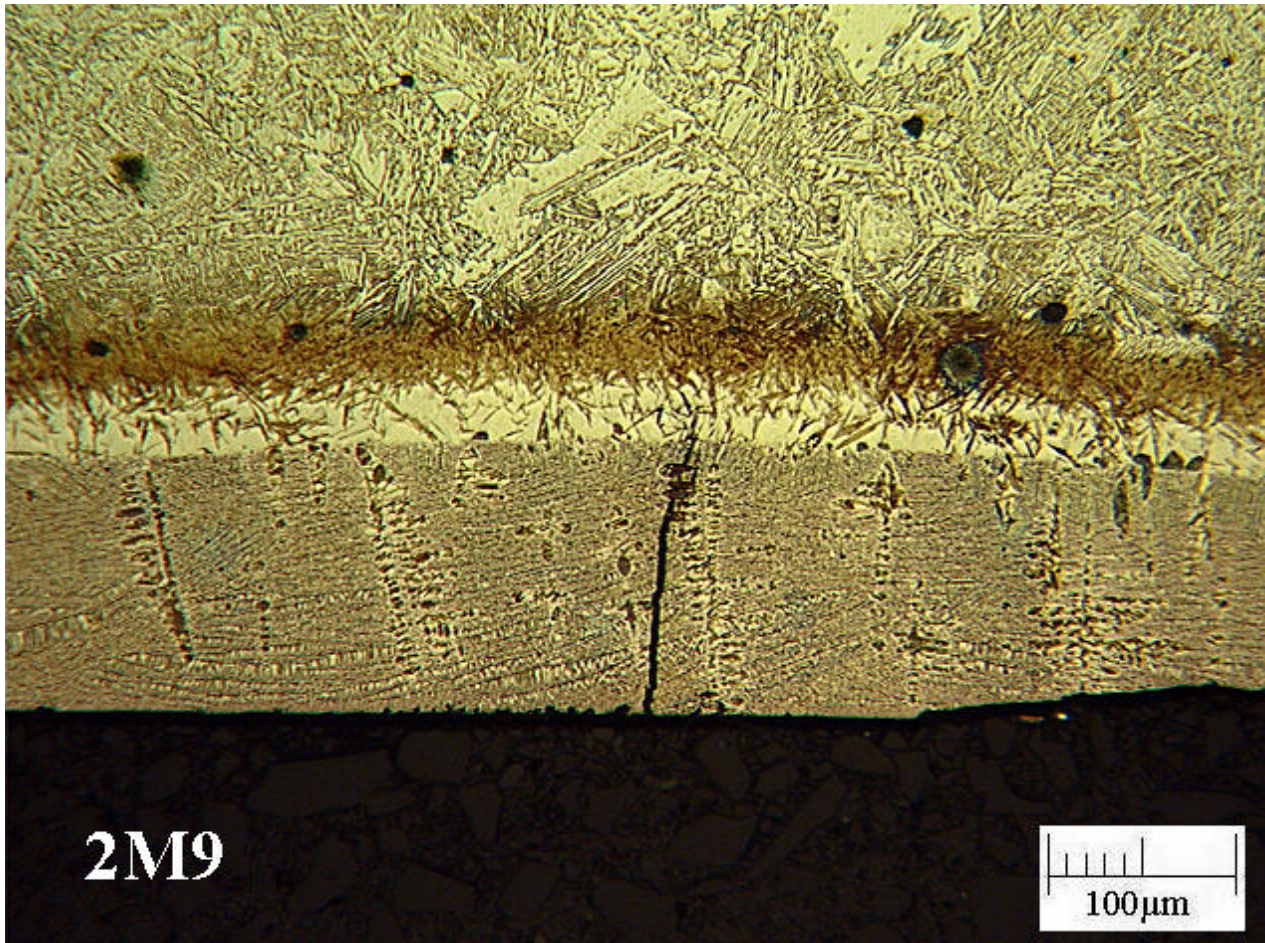
Figure 82 - Cracks in Eutectic Iron Layer of Metallographic Section Shown in Figure 81

In a field repair situation, evacuating a pipeline prior to weld repair will be particularly difficult. There is a high probability that the weld shielding gas will be contaminated to some degree with methane that remains in the pipe; therefore, EWI conducted weld trials with a shielding gas containing various levels of methane to determine the effect of methane on resultant weld quality. Table 15 contains the volume percent of methane for each weld specimen. Each weld was cross-sectioned and three weld metal hardness values obtained. The chemical composition of each weld were also measured to determine if the presence of methane affected the carbon content of each deposited weld.

Weld ID	Shielding Gas Flow Rate				Volume Percent Methane	Average Weld Metal Hardness (Hv-10kg)	Weld Metal Carbon Content (%)	Comments
	95% Ar + 5% CO_2		10% Methane + 4.5% CO_2 + 85.5% Ar					
	(m^3/hr)	(ft^3/hr)	(m^3/hr)	(ft^3/hr)				
325-2	1.42	50	0.00	0	0.0	169.7	0.073	No Porosity
325-3	1.13	40	0.28	10	2.0	174.7	0.074	No Porosity
325-4	0.99	35	0.42	15	3.0	175.0	0.062	Porosity
325-5	0.85	30	0.57	20	4.0	175.3	0.071	Porosity
325-6	1.22	43	0.20	7	1.4	169.7	0.075	No Porosity
325-8	0.99	35	0.28	10	2.2	176.7	0.071	No Porosity
325-9	0.85	30	0.42	15	3.3	171.3	0.081	Porosity

Table 15 - Volume Percent of Methane per Weld Specimen

The average weld metal hardness values and percent carbon content from Table 15 are graphically depicted in Figure 83.
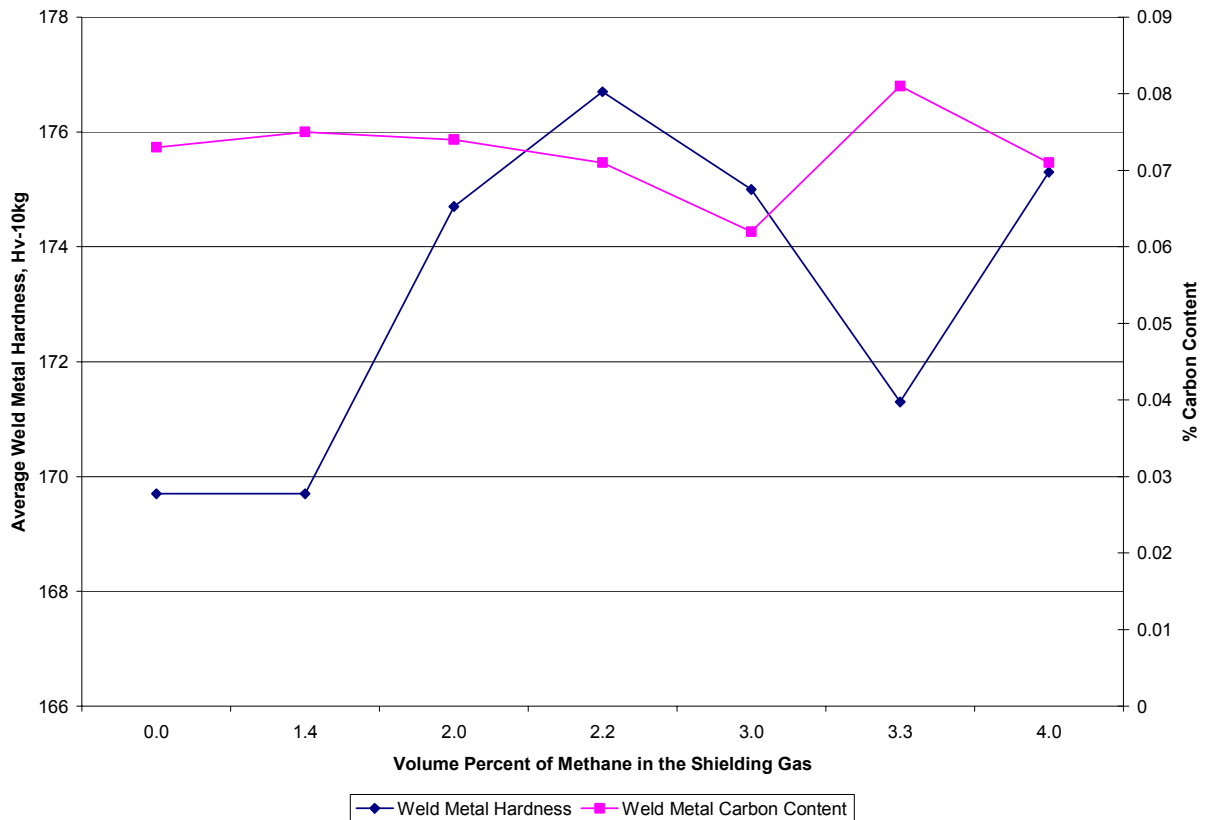
Figure 83 - Graphical Representation of Table 15 Hardness Values and Carbon Content

In Figure 83, the weld metal hardness scale is on the left axis and the percent carbon content of the weld metal is shown on the right axis. Increasing the volume percent of methane did not consistently increase either weld metal hardness or percent carbon content of the weld metal.

Each weld deposit specimen (made in methane) was photographed as shown in Figure 84 through Figure 90. A visual examination of the samples revealed that a volume of 3% methane caused porosity in weld specimens 325-4 (Figure 86), 325-5 (Figure 87), and 325-9 (Figure 90).

Figure 84 - Weld Specimen 325-2

Figure 85 - Weld Specimen 325-3

Figure 86 - Weld Specimen 325-4

Figure 87 - Weld Specimen 325-5

Figure 88 - Weld Specimen 325-6

Figure 89 - Weld Specimen 325-8

Figure 90 - Weld Specimen 325-9

These results clearly indicate that an increased volume of methane in the weld shielding gas produces welds with porosity defects that decrease weld quality. Adequate shielding gas protection is critical to creating sound, defect free welds. Providing adequate gas shielding protection during welding will be extremely difficult to achieve in a field repair situation.

The results of these trials indicate that the use of weld deposition, although promising in principal, is less than ideal for internal repair of gas transmission pipelines. While weld deposition repairs applied to the outside of exposed pipelines are becoming more commonplace in the gas transmission pipeline industry, the application of this technique to the inside of the

pipe presents a number of difficulties. When applied to the outside of an exposed pipeline, dents or concavity that result from welding residual stresses can be overcome by simply applying more weld metal until the outside diameter of the pipe is restored. This is not possible for internal repair where additional weld metal would result in further concavity. In addition to the difficulties that arise from remotely operating welding equipment from great distances, the presence of methane in the welding environment would seem likely to cause additional difficulties.

Baseline Pipe Material Performance

Because of the large discrepancies in the predicted burst pressures and the actual burst pressures, additional physical testing was performed.

Four hydrostatic pressure tests were conducted for pipe sections in the following pipe materials and conditions:

- 558.8 mm (22 in.) diameter by 7.92 mm (0.312 in.) thick API 5L Grade B pipe sections:
    - Virgin condition
    - Un-repaired with simulated corrosion damage
- 508.0 mm (20 in.) diameter by 6.35 mm (0.25 in.) wall API 5LX-52 pipe sections:
    - Virgin condition
    - Un-repaired with simulated corrosion damage

A section of the pipe material was also taken from each pipe diameter to determine the actual material strengths. Table 16 contains the resultant tensile and yield strengths of the two pipes. The tensile strength was then used to determine the corresponding burst pressures found in Table 17.

Pipe Diameter mm (in.)	Specimen		Ultimate Strength	0.2% Yield Strength	Elongation %	Reduction of Area %
	Width	Thickness				
	mm (in)	mm (in)	MPa (ksi)	MPa (ksi)		
508.0 (20)	38.1 (1.5)	6.6 (0.26)	601.4 (87.2)	462.8 (67.1)	29.9	58.5
558.8 (22)	38.1 (1.5)	7.87 (0.31)	384.8 (55.8)	238.6 (34.6)	40.3	65.0

Table 16 - Tensile and Yield Strengths of the 508 mm (20 in.) and 558.8 mm (22 in.) Pipe

Table 17 is a summary of the results of all the RSTRENG calculations and the calculated burst pressure from 100%SMYS and the tensile strength of the pipe.

Pipe Outside Diameter	558.80 mm (22 in.)	508 mm (20 in.)
Wall Thickness	7.92 mm (0.312 in.)	6.35 mm (0.250 in.)
Pipe Material	API 5L-Grade B	API 5L-X52
Type of Damage	Simulated Corrosion Defect	Simulated Corrosion Defect
Damage Length	190.50 mm (7.5 in.)	127.00 mm (5 in.)
Damage Depth	3.96 mm (0.156 in.)	3.45 mm (0.136 in.)
Pressure corresponding to 100% SMYS	6.84 MPa (992 psi)	8.96 MPa (1,300 psi)
Damage as % of wall thickness	50%	54%
RSTRENG-predicted burst pressure compared to pressure at 100% SMYS	75%	75%

Table 17 - Calculated Values for Simulated Damage for 508 mm (20 in.) and 558.8 mm (22 in.) Pipe

Figure 91 through Figure 94 contain photos of the hydrostatic test specimens without repairs.

Figure 91 - Hydrostatic Burst Specimen of 508.0 mm (20 in.) in Virgin Pipe

Figure 92 - Hydrostatic Burst Specimen of 508.0 mm (20 in.) with Un-Repaired Damage

Figure 93 - Hydrostatic Burst Specimen of 558.8 mm (22 in.) Pipe in Virgin Pipe

Figure 94 - Hydrostatic Burst Specimen of 558.8 mm (22 in.) With Un-Repaired Damage

Table 18 contains the predicted and actual burst pressures for all six hydrostatic tests during this reporting period. Measured burst pressure for pipe with un-repaired corrosion damage was 85% of the measured burst pressure for pipe in the virgin condition in 558.80 mm (22 in.) diameter pipe and 91% for 508 mm (20 in.) pipe.

Pipe Diameter	Pipe Condition	Predicted Burst Pressure		Actual Burst Pressure	
		(MPa)	(psi)	(MPa)	(psi)
508.0 mm (20 in.)	Virgin	10.91	1,583	16.03	2,325
	Simulated Damage Un-Repaired	6.72	974	14.57	2,112
	Simulated Damage Repaired with Carbon Fiber-Reinforced Liner	-	-	15.13	2,194
558.8 mm (22 in.)	Virgin	15.03	2,180	12.70	1,842
	Simulated Damage Un-Repaired	5.15	747	10.78	1,563
	Simulated Damage Repaired with Weld Deposition	-	-	9.68	1,404

Table 18 - Summary of Predicted vs. Actual Hydrostatic Burst Pressure Values

41633R47.pdf

Not surprisingly, the specimens of virgin pipe material had the highest hydrostatic burst pressures. The most surprising characteristic about the hydrostatic burst test results is that the failure pressures for the pipe sections with un-repaired damage are significantly greater than the RSTRENG predicted burst pressures. The areas of damage were designed using RSTRENG to produce a 25% reduction in predicted burst pressure (i.e., designed to require repair according to RSTRENG). For the 508.0 mm (20 in.) diameter pipe, the reduction in burst pressure that resulted from introducing the simulated corrosion damage, which was 127 mm (5 in.) long and more than 50% of the pipe wall thickness deep, is only 9% as opposed to the predicted 25%.

The pipe section with simulated corrosion damage repaired with a carbon fiber-reinforced liner had a burst pressure that was greater than the pipe section with un-repaired damage. By contrast, the pipe section with simulated corrosion damage repaired with weld deposition had a burst pressure that was less than the pipe section with un-repaired damage. Distortion caused by welding residual stresses may have contributed to the lower burst pressure. Of the two potential pipeline repair technologies evaluated this reporting period, carbon fiber-reinforced liner repair was generally more effective at restoring the pressure containing capability of a pipeline.

The results of these experiments illustrate that RSTRENG predictions tend to be conservative.[9] This conservatism will be taken into account in future experiments by designing and introducing areas of damage that have significantly larger predicted reductions in burst pressure (e.g., 50% as opposed to 25%). This will allow the ability of repairs to restore pressure containing capability to be better demonstrated.

5.0 - CONCLUSIONS

The most common cause for repair of gas transmission pipelines is external, corrosion-caused loss of wall thickness[10]. To prevent an area of corrosion damage from causing a pipeline to rupture, the area containing the corrosion damage must be reinforced. Other pipeline defects that commonly require repair include internal corrosion, original construction flaws, service induced cracking, and mechanical damage.

Defects oriented in the longitudinal direction have a tendency to fail from hoop stress (pressure loading) and must be reinforced in the circumferential direction. Defects oriented in the circumferential direction have a tendency to fail from axial stresses (due to pipeline settlement, etc.) and must be reinforced in the longitudinal direction. Full-encirclement steel repair sleeves resist hoop stress and, if the ends are welded to the pipeline, can also resist axial stresses.

Fiber-reinforced composite liner and weld metal deposition repair technologies were evaluated by this program. Both are used to some extent for other applications and could be further developed for internal, local, structural repair of gas transmission pipelines.

Fiber-reinforced liner repair is contemplated most often for external corrosion that exceeds the allowable limit sizes, corrosion on the external surface may continue after the emplacement of the liner. Engineering analysis determined that a high fiber modulus and a high shear strength of the matrix (above that for many thermoplastics) is required for composite liners to resist the types of shear stresses that can occur when external corrosion continues to the point where only the liner carries the stresses from the internal pressure in the pipe. Realistic combinations of composite material and thickness were analytically determined for use in a carbon fiber-reinforced liner system.

Failure pressures for pipe sections repaired with a circumferential glass fiber-reinforced composite liners were only marginally greater than that of pipe sections without liners, indicating that the glass fiber-reinforced liners are generally ineffective at restoring the pressure containing capabilities of pipelines.

Arc welding processes offer a repair method that can be applied from the inside of a gas transmission pipeline. There are several arc welding processes that can be operated remotely. Based on the survey and assessment of candidate arc welding processes, the GMAW process was the most likely choice for this application. It offers a good combination of simplicity, high productivity, robustness, and quality that are required for this welding repair application. Arc welding processes are routinely used to externally repair pipelines. However, repair from the inside offers new challenges for process control since welding would need to be performed remotely. In addition, since the intent is to leave the pipeline in the ground, there are several

variables that will affect the welding process and quality. Soil conditions have the potential to influence heat removal during welding thereby altering the fusion characteristics, welding cooling rate, and resultant mechanical properties. The effects of welding on the external coating used to protect against corrosion would also need thorough evaluation to assure future pipeline coating integrity. Finally, if welding is performed in-service, the pressure and flow rate of the gas would have a strong effect on the equipment design of the welding process. New process equipment technology would be required to shield the welding process from methane contamination and to cope with higher gas pressures in-service. The development of an equipment specification defining all the functional requirements for an internal welding repair system would require significant effort.

In addition to the previously stated characteristics of a useful internal pipeline repair system, a successful internal welding repair system would need a machining capability to prepare the weld joint, a grinding system for cleaning and preparation, in addition to a robust, high deposition welding process. Although many of these features are incorporated in existing pigging systems, there is no single system that possesses all the required characteristics. Further work is required to develop a system with all of these features.

Specimens of virgin pipe material had the highest hydrostatic burst pressures. The pipe section with simulated corrosion damage repaired with a carbon fiber-reinforced liner had the next highest burst pressure. The specimens of un-repaired pipe with simulated corrosion damage had the third highest burst pressures. The pipe section with simulated corrosion damage repaired with weld deposition exhibited the lowest burst pressure.

Testing conducted clearly indicates that carbon fiber-reinforced liner repair is the most promising technology evaluated to-date. Development of a comprehensive test plan for this process is recommended for use in the field trial portion of this program.

6.0 - REFERENCES

(1)   Kiefner, J. F. and Vieth, P. H., "A Modified Criterion for Evaluating the Remaining Strength of Corroded Pipe" Final Report to A.G.A. Pipeline Corrosion Supervisory Committee, Project PR-3-805, Battelle, Columbus, OH, December 1989.

(2)   Gordon, J. R., Bruce, W. A., and Porter, N. C., "Internal Repair of Pipelines – Research Management Plan," Report to National Energy Technology Laboratory, U.S. Department of Energy, DOE Award No.: DE-FC26-02NT41633, Edison Welding Institute, October 2002.

(3)   Gordon, J. R., Bruce, W. A., Sullivan, M., and Neary, C. M., "Internal Repair of Pipelines – Technology Status Assessment," Report to National Energy Technology Laboratory, U.S. Department of Energy, DOE Award No.: DE-FC26-02NT41633, Edison Welding Institute and Pacific Gas & Electric, November 2002.

(4)   U. S. Department of Transportation, Research and Special Programs Administration, "§192.150 Passage of internal inspection devices," DOT 49 CFR Part 192 - Transportation of Natural & Other Gas by Pipeline: Minimum Safety Standards, July 1998.

(5)   U. S. Department of Transportation, Research and Special Programs Administration, Office of Pipeline Safety, "Pipeline Failure Causes," *http://primis.rspa.dot.gov/pipelineInfo/stat_causes.htm* (Washington, DC: U. S. Department of Transportation, Research and Special Programs Administration, Office of Pipeline Safety, 17 June 2004)

(6)   Wang, Y.-Y., and Bruce, W. A., "Examination of External Weld Deposition Repair for Internal Wall Loss," Final Report for EWI Project No. 07723CAP to PRC International, Contract No PR-185-9633, March 1998.

(7)   Bruce, W. A., "Welding onto In-Service Thin Wall Pipelines," Final Report for EWI Project No. 41732CAP to PRC International, Contract No PR-185-9908, July 2000.

(8)   Kiefner, J. F., Barnes, C. R., Gertler, R. C., Fischer, R. D., and Mishler, H. W., "Experimental Verification of Hot Tap Welding Thermal Analysis. Final Report - Phase II - Volume 2, Liquid Propane Experiments," Repair and Hot Tap Welding Group, Battelle Columbus Laboratories, May 1983.

(9)   Kiefner, J. F., Private communication, Kiefner & Associates, July 2004.

(10) Eiber, R. J., Bubenik, T. A., and Leis, B. N., "Pipeline Failure Mechanisms and Characteristics of the Resulting Defects," Eighth Symposium on Line Pipe Research, Paper No. 7 (Houston, TX: American Gas Association, 1993).

7.0 - BIBLIOGRAPHY

Kiefner, J. F. and Vieth, P. H., "A Modified Criterion for Evaluating the Remaining Strength of Corroded Pipe" Final Report to A.G.A. Pipeline Corrosion Supervisory Committee, Project PR-3-805, Battelle, Columbus, OH, December 1989. This report documents a modified criterion for evaluating the corrosion level of a pipeline based on pipeline stress calculations (available as a PC program) as a less conservative alternative to ANSI / ASME B31G.

Gordon, J. R., Bruce, W. A., and Porter, N. C., "Internal Repair of Pipelines – Research Management Plan," Report to National Energy Technology Laboratory, U.S. Department of Energy, DOE Award No.: DE-FC26-02NT41633, Edison Welding Institute, October 2002. This plan contains a concise summary of the technical objectives and approach for each task. The document also contain detailed schedules and planned expenditures for each task and all major milestones and decision points for the two year project duration.

Gordon, J. R., Bruce, W. A., Sullivan, M., and Neary, C. M., "Internal Repair of Pipelines – Technology Status Assessment," Report to National Energy Technology Laboratory, U.S. Department of Energy, DOE Award No.: DE-FC26-02NT41633, Edison Welding Institute and Pacific Gas & Electric, November 2002. This report presents the status of existing pipeline repair technology that can be applied to the inside of gas transmission pipelines, and includes results from a comprehensive computerized literature search, together with information obtained from discussions with companies that are currently developing or evaluating novel pipeline repair methods.

U. S. Department of Transportation, Research and Special Programs Administration. "§192.150 Passage of internal inspection devices." *DOT 49 CFR Part 192 - Transportation of Natural & Other Gas by Pipeline: Minimum Safety Standards*. Amdt. 192-72, 59 FR 17281, Apr 12, 1994, as amended by Amdt. 192-85, 63 FR 37502, July 13, 1998. This code describes minimum safety requirements for pipeline facilities and the transportation of gas, including pipeline facilities and the transportation of gas within the limits of the outer continental shelf as that term is defined in the Outer Continental Shelf Lands Act (43 U.S.C. 1331).

U. S. Department of Transportation, Research and Special Programs Administration, Office of Pipeline Safety, "Pipeline Failure Causes," *http://primis.rspa.dot.gov/pipelineInfo/stat_causes.htm* (Washington, DC: U. S. Department of Transportation, Research and Special Programs Administration, Office of Pipeline Safety, 17 June 2004). This web site provides comprehensive information about the U.S. transportation pipeline infrastructure. It is developed and maintained by

the Office of Pipeline Safety (OPS) of the U.S. Department of Transportation's Research and Special Programs Administration.

Wang, Y.-Y., and Bruce, W. A., "Examination of External Weld Deposition Repair for Internal Wall Loss," Final Report for EWI Project No. 07723CAP to PRC International, Contract No PR-185-9633, March 1998. This report discusses the deposition of weld metal on the external surface of straight sections of pipe, field bends, tees and elbows as a potentially useful method for in-service repair of internal wall loss.

Bruce, W. A., "Welding onto In-Service Thin Wall Pipelines," Final Report for EWI Project No. 41732CAP to PRC International, Contract No PR-185-9908, July 2000. This report discusses special welding difficulties and the extra care required to ensure safe operating procedures and sound welds due to repairs and modifications to in-service, thin walled pipelines.

Kiefner, J. F., Barnes, C. R., Gertler, R. C., Fischer, R. D., and Mishler, H. W., "Experimental Verification of Hot Tap Welding Thermal Analysis. Final Report - Phase II - Volume 2, Liquid Propane Experiments," Repair and Hot Tap Welding Group, Battelle Columbus Laboratories, May 1983. This report documents the verification of two thermal analysis models of hot tap welding on pressurized pipelines. With velocity input modified as shown, the models are capable of predicting maximum temperatures in the pipe wall especially at the inside surface and critical cooling rates in the heat-affected zones within the range of heat inputs that are practical for shielded metal arc welding.

Kiefner, J. F., Private Communication, Kiefner & Associates, July 2004. This conversation was a discussion of the theory upon which the RSTRENG software is based.

Eiber, R. J., Bubenik, T. A., and Leis, B. N., "Pipeline Failure Mechanisms and Characteristics of the Resulting Defects," Eighth Symposium on Line Pipe Research, Paper No. 7 (Houston, TX: American Gas Association, 1993). This report discusses four broad categories of pipeline failure mechanisms: outside forces, environmentally induced defects, manufacturing/materials defects, and operator error or miscellaneous defects.

8.0 - LIST OF ACRONYMS

ANSI	American National Standards Institute
API	American Petroleum Institute
ASME	American Society of Mechanical Engineers
CAE	Computer Aided Engineering
CP	Cathodic Protection
CRLP	Composite Reinforced Line Pipe
CSA	Canadian Standards Association
CV	Constant Voltage
DOE	Department of Energy
DOT	Department of Transportation
ERW	Electric Resistance Welded
EWI	Edison Welding Institute
FBE	Fusion Bonded Epoxy
FEA	Finite Element Analysis
FRCP	Fiber-Reinforced Composite Pipe
Glass-HDPE	Glass-High Density Polyethylene
GMAW	Gas Metal Arc Welding
HDD	Horizontal Direct Drilling
HDPE	High Density Polyethylene
ILI	In-Line Inspection
IR	Infra-Red
MAOP	Maximum Allowable Operating Pressure
MOP	Maximum Operating Pressure
MPI	Magnetic Particle Inspection
NDE	Nondestructive Examination
NETL	National Energy Technology Laboratory
OD	Outside Diameter
PC	Personal Computer
PE	Polyethylene
PG&E	Pacific Gas & Electric Co.
PRCI	Pipeline Research Council International
QA	Quality Assurance
QC	Quality Control
RT	Radiographic Testing
SCC	Stress Corrosion Cracking
SMYS	Specified Minimum Yield Strength
UT	Ultrasonic Testing
MEKP	Methyl Ethyl Ketone Peroxide
VARTM	Vacuum Assisted Resin Transfer Molding